university of groningen / faculty of mathematics and natural sciences

The influence of Wall Teichoic Acids on cell viability and morphology in *Bacillus subtilis*

by

Jan Wintgens (S2504618)

Master research Project I

November 2014

Supervision:

Marielle van den Esker

Prof. Dr. O.P Kuipers

Abstract

Wall teichoic acids (WTA's) are negatively charged polymers that play an important role in the cell envelope. Among other functions they are influencing cell morphology and autolysin activity. The mechanism of the latter is only shown in *Staphylococcus aureus* and is poorly understood. We here show the impact on morphology by WTA's in detail and started investigating the role of WTA's in lysis in *Bacillus subtilis.* Lacking the first step in WTA biosynthesis the *ΔtagO* conditional knockout mutant was used to characterise growth under different wall teichoic acid concentrations. We found that growth is generally impaired and initially cannot be complemented to WT level. The mutant however, surprisingly regrows after a lysis phase of diverging length, a phenomenon that requires further investigation. Measuring the morphology of the mutant, we were able to show in a detailed length to width ratio analysis that WTA are important to maintain the rod shape of the bacteria. We also detected an increase of volume by up to 330% caused by the lack of WTA's. Both results show that wall teichoic acids are a structure that is partially responsible for cell shape maintenance in gram positive bacteria. A difference in charge or size between WTA in the WT and in the mutant is apparent in our results. It gives insight in the reaction of the cell to a lack of WTA's and the regulation of their biosynthesis. It also has an impact on all other results we obtain with this mutant. Finally we were able to show that WTA's are responsible for up to 23% of the cation binding capacity in the cellular envelope of *Bacillus subtilis*. This result is similar to the ones achieved using *Staphylococcus aureus*, in which it has been shown that this influences autolysin activity.

Table of Contents

Introduction

The Cell Envelope

The cell envelope of bacteria is a complex structure that shows a great variety in composition and the functions it fulfils, like maintaining cell shape and interaction with the exocytoplasm[1]. The absence of an outer membrane in gram-positive bacteria, like the here studied *Bacillus subtilis 168* is one of the main differences compared to gram-negative ones, in which two membranes create the periplasm[2]. This compartment filters toxic molecules and serves as an anchoring scaffold for proteins involved in respond systems to the environment. Functions fulfilled by this outer membrane have to be replaced by structures present in and bound to the peptidoglycan (PG) matrix, the dominant component of gram-positive cell envelopes(Figure 1)[3].

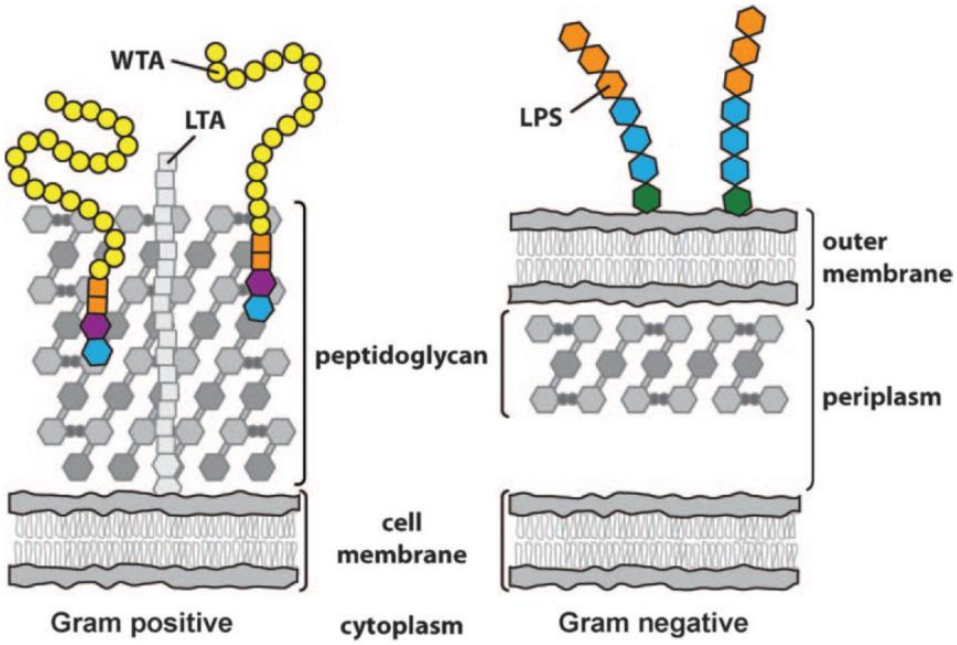

Figure 1: Schematic overview of gram positive and gram negative cell envelopes. In contrast to gram-negative organisms, gram-positive organisms do not show a distinct periplasm . Proteins are not shown. LTA: lipoteichoic acid; LPS: lipopolysaccharide; WTA: wall teichoic acid [2].

Peptidoglycan is a cross-linked matrix of glycan chains. This carbohydrate network is linked to one another via covalently bound peptide side chains[4]. In gram-positive bacteria the layer is especially thick and its organization serves several purposes, such as binding proteins as well as other components and withstanding high internal osmotic pressure. The cell wall of *Bacillus subtilis* for example defies a pressure of approximately 2.43 bar compared to 0.5 of the one of *E.coli* (gram-negative)[5].

The architecture of PG is differing between bacterial strains[5]. In general, PG consists of strands made from two alternating amino sugars, namely N-acetylglucosamine (GlcNAc or NAG) and N-acetylmuramic acid (MurNAc or NAM). The strands are linked by a 4-5 residue amino acid unit between the chains.

Different polymers are linked to the peptidoglycan. Most abundant are carbohydrate based anionic strands, called teichoic acids. In concert with the peptidoglycan, teichoic acids create a polyanionic network that contributes to many attributes such as: tensile strength, elasticity, porosity and electrostatic steering of the cell envelope[6]–[9]. The influence of especially the wall teichoic acids on the cell envelope and its proposed functions will be elucidated in this report in greater detail.

With up to 60% of the cell wall mass, teichoic acids play a major role in the composition and function of the extracytoplasm[10]. Two types of teichoic acids can be differentiated; there are lipoteichoic acids (LTA) and the aforementioned wall teichoic acid (WTA). LTAs are linked to a glycolipid anchor unit that attaches them to the cell membrane, from where they extend into the peptidoglycan layer[11]. WTAs are covalently linked to the peptidoglycan from where they expand through the cell wall and beyond it. It is unclear how much further the wall teichoic acids are stretched beyond the PG[12]. It has been estimated that every ninth PG MurNAc residue has a WTA Polymer attached to it, creating a dense network[13]. Both polymers are rich in phosphor and create a negatively charged environment from the bacterial cell membrane till the outer parts of the cell wall (Figure 2). If grown under phosphate limited conditions *Bacillus subtilis* switches from building teichoic acids to teichuronic acids, a heteropolymeric polysaccharide containing uronic acid and carbohydrates, but no phosphor[14]. Their biosynthesis is up-regulated strictly only under phosphate limited conditions[15]. It goes along with up-regulation of enzymes for increased phosphate uptake and degradation of teichoic acids, to maintain the level of phosphor in the cytoplasm in order to sustain e.g DNA synthesis[16].

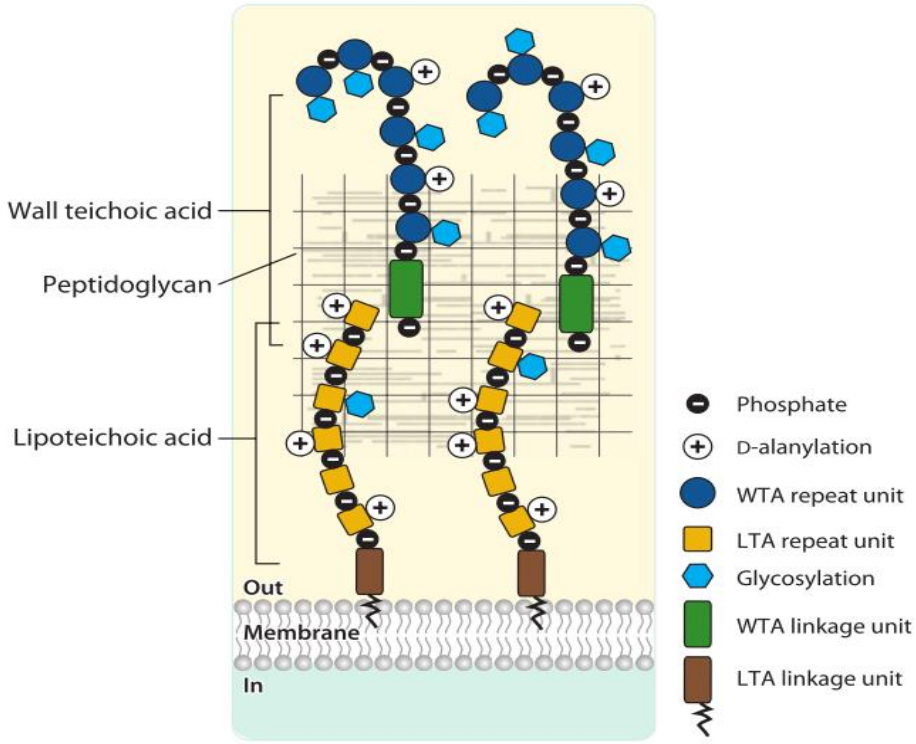

Figure 2: Location of teichoic acids in the gram positive cell wall. Lipoteichoic acids (LTA, yellow) are anchored to the membrane, wall teichoic acids (WTA, blue) are covalently attached to the peptidoglycan (PG, grey)[17].

Wall Teichoic Acid Structure

The polymer creating a wall teichoic acid can be divided in two main components; a disaccharide linking unit, and the main polymer, a phosphodiester-linked polyol repeat unit (Figure 3) [17]. The linkage unit is conserved over species and therefore also over different types of WTA's. The GlcNAc unit of the linker is covalently connected to the C4 Oxygen of MurNAc, the second linkage unit building block, by one or two glycerol 3-phosphate units[13]. The C6 hydroxyl in the PG's MurNAc is bound to the anomeric phosphate of the linkage unit by a phosphodieseter bond. On the other side of the anchor a GroP unit connects to the phosphodiester-linked polyol repeat unit(Figure 3) [3].

In *Bacillus subtillis 168* the repeat unit comprises a glycerol 3-phosphate (GroP). *Bacillus subtillis W23* and *Staphylococcus aureus* contain a ribitol 5-phosphate (RboP) repetition unit. The two mentioned units are most common, but other compositions are also present among other species. All variations share common functions and a negatively charged anionic backbone(Figure 3). GroP however is abundant in phosphor content compared to the other variations. It has less side chains and less carbon atoms between the phosphor groups, which increases the density of phosphor in comparison to other polymers[18].

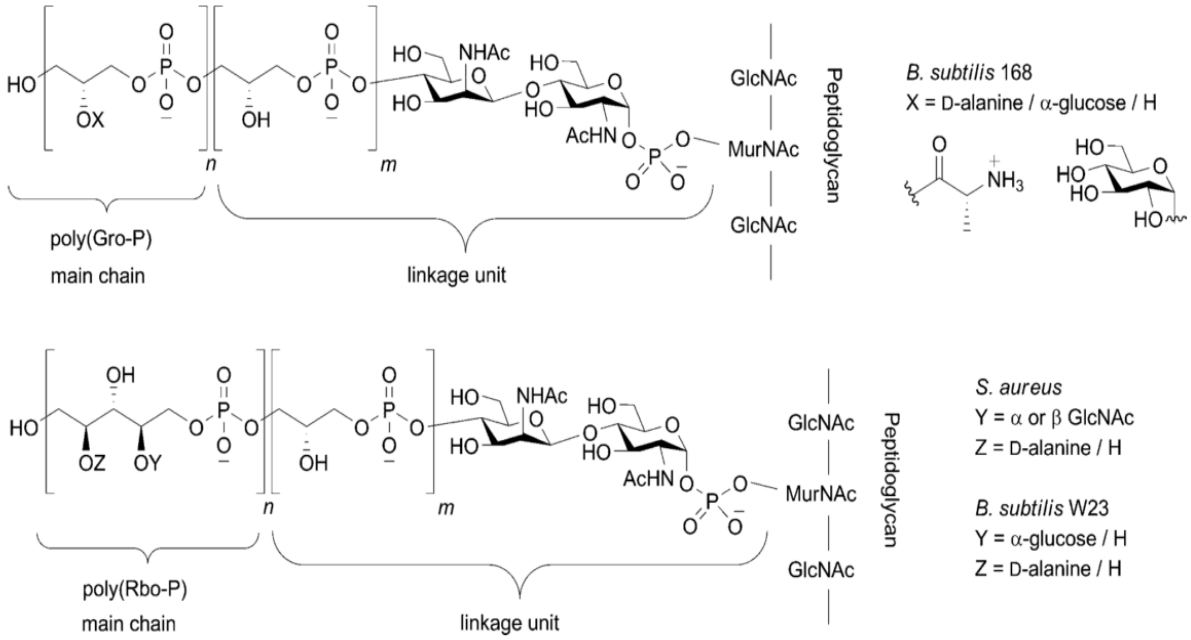

Figure 3: Chemical structures of WTA's from *Bacillus subtilis* and *Staphylococcus aureus*. (m = 1–3 and n = 20–40)[2].

Wall Teichoic Acids Biosynthesis

Intracellular assembly

The biosynthesis of WTA's takes place at the wall-membrane interface, which is located in the cytoplasm[14]. In *Bacillus subtilis* the here described Poly(GroP) WTA synthesizing proteins are encoded by the *tag* genes (**t**eichoic **a**cid **g**lycerol). TagO is responsible for catalysing the first step, in which the membrane anchored undecaprenyl phosphate carrier lipid is loaded with GlcNAc-1-P from UDP-GlcNAc (N-acetylglucosamine). The carrier lipid is an intermediate shared with PG biosynthesis[19]. TagA then further transforms the linkage unit, which transfers ManNAc from UDP-ManNAc to the C4 hydroxyl of GlcNAc. A glycerophosphotransferase encoded by *tagB* concludes the three step synthesis of the WTA linkage unit. In particular, it catalyses the transfer of a GroP unit from CDP-glycerol to the C4 position of ManNAc[20]. The linkage unit assembly is a highly conserved pathway, in all strains characterised to date (Figure 4A). TagF is the next enzyme in line, responsible for assembling the polymer's 45 – 60 glycerol-phosphate units by adding them to the aforementioned linker. To prepare the units for polymerisation, a cytidylyltransferase, encoded by *tagD*, catalyses the transfer of L-α-glycerol 3-phosphate to CTP by releasing a pyrophosphate (Figure 4B) [21].

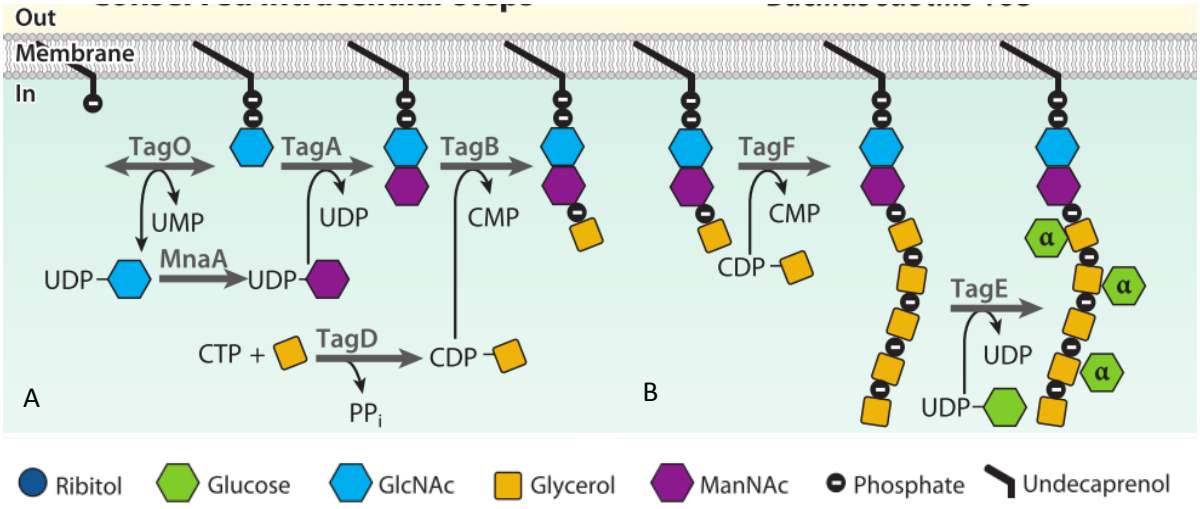

Figure 4: WTA Biosynthesis(A) Assembly of the linkage unit, conserved in all too date characterized pathways (B) *Bacillus subtilis* specific assembly of polymer. Abbreviations: GlcNAc, N-acetylglucosamine; ManNAc, N-acetylmannosamine;WTA, wall teichoic acid and CTP, cytidine triphosphate[17].

Tailoring modifications of WTA's

tagE codes for a protein modifying WTA's with α-glucose, using UDP-glucose as a substrate[22]. One strand is either heavily modified with sugars of the same stereochemistry or not altered at all[23]. The structure of the polymer is influenced by the modification, which changes its interaction with other components in- and outside the cell wall[17]. Another tailoring modification on the WTA's is D-alanylation. The *dlt* operon is responsible for the catalyzation. DltA activates D-alanine to its corresponding aminoacyl adenylate. This compound is then attached to DltC, which is transported through the membrane, presumably with the help of DltB and DltD[24]. The occurrence of this modification has been shown to be affected by e.g. growth media, pH and temperature[4]. The D-alanylation adds an ester to the teichoic acid that provides a positive charge to them, resulting in a zwitterion. It reduces repulsion between the strongly negatively charged acids and enhances ion pair formation between cationic esters and anionic phosphate groups[25].

Polymer export

As the assembly and polymerization takes place inside the cytoplasm, the WTA strands have to be transported through the membrane to reach their designated location. This happens by a two-component ATP-binding cassette (ABC transporter). The genes that are coding for this ABC transporter are termed as *tagGH*. The energy needed to perform a conformational switch in TagH is provided by TagG, which contains an ATPase domain. This conformational switch leads to a

translocation of the molecule across the membrane[26][27]. The exact mechanism remains to be elucidated but it is suggested that a flipping of the anchoring unit is initiated. This movement then drags the polymer chain out of the cytoplasm bottom first, with the top following last. The suggested movement is supported by findings that show recognition of the linking unit and not the main chain as a reaction partner by TagGH[26].

The final step of the synthesis is the linking of the polymer to the PG. As mentioned before, the WTA's are connected to the C6 hydroxyl of the MurNAc unit in the PG. The gene cluster *tagTUV* is responsible for catalysing this particular coupling reaction[28]. Whether the connection is made to nascent or old peptidoglycan still needs to be investigated, this also holds true for the exact mode of action by the mentioned genes. It is only known that *tagT* codes for a geranyl pyrophosphatase activity[28], how this is influencing the coupling in particular remains unclear to date.

Necessity and conditional necessity of *tag* genes

Of the mentioned biosynthesis genes only *tagO* was shown to be non-essential[29]. Additionally all tailoring enzymes are non-essential. However, most of the downstream WTA biosynthesis related genes are essential (*tagADF*), if the upstream process is not interfered with[29]. This might be connected to the accumulation of toxic intermediates[30].

Roles of Wall Teichoic Acids

The functions of wall teichoic acids are not well understood. The amount of WTA's in the cell envelope suggests that they play a role in almost every function it fulfils.

Regulation of Ion Homeostasis

Binding of extracellular metal cations is highly influenced by wall teichoid acids. By extending beyond the PG layer, as mentioned earlier, the anionic backbone binds to the positively charged metal. In *Staphylococcus aureus* wall teichoic acid biosynthesis has been shown to be upregulated when grown in cation limited media[31]. The D-alanylation tailoring decreases the cation binding effect by adding a positive charge to the tip of the polymer. Independent from that, when lacking WTA's, *Staphylococcus aureus* has a 23% decrease in the binding of protons[17]. Another proposed function of wall teichoic acids binding cations is that this minimizes repulsion between the phosphate groups. This can affect polymer structure and cell wall integrity, especially due to their density in the cell envelope[32].

Regulation of cell morphology and division

Bacillus subtilis with defects in WTA biosynthesis grow slower than the wild type[33]. These strains are also showing morphological abnormalities. A transformation to a spherical in contrast to the wild types natural rod shape is reported[34], but not analysed in detail. The peptidoglycan layer is shown to be of inconsistent thickness[34]. Other findings, such as defects in the septal positioning or increased cell size have been linked to missing WTA's in other organisms[17]. These findings give reason to hypothesize that wall teichoic acids play a major role in cell wall assembly and renewal, which is important for cell division. Co-localisation and interaction of PG and WTA biosynthetic enzymes have been reported and support this hypothesis[28]. Especially the enzymes with autolytic activity are believed to be regulated by WTA's[35]. Autolysins are responsible for hydrolysis of the PG. If their regulation is impaired this could lead to a higher lysis rate.

Linking the presence of wall teichoic acids to autolytic activity is, to date, mainly shown in *Staphylococcus aureus*[17]. Studies support an interaction between the autolysins and WTA's driven by the strong charges in the WTA polymer. Autolytic enzymes in *Bacillus subtilis* however are often different in mode of action and structure from those in *Staphylococcus aureus*[36]. Still, the structural circumstances and similarities in the cell envelope ask for further investigation[25]. A proposed model of interaction, in gram positive bacteria, is the influence on autolysis by ion chelation with WTA's. This could lead to several interactions with the autolytic enzymes. It has been shown in *Staphylococcus aureus* that autolysins can be influenced by even slight changes in the pH, or in the proton gradient. Both can be linked to the presence of anionic polymers by ion chelation. Especially diverging ion binding of the anionic network is believed to create regional changes in the pH[35].

Purpose and experimental setup

In this study cell growth and morphology in a *Bacillus subtilis* 168 mutant with regulated wall teichoic acid expression was examined.The gene product of *tagO* catalyses the initial step of WTA synthesis, making the ΔtagO mutant lacking the entire WTA polymer[17]. WTA's could be reintroduced by an inducible promoter. This enabled us to investigate growth, corresponding morphology, PG occurrence and cation binding under diverging WTA conditions. We compared the influence of *tagO* to that of other mutants, to confirm that the obtained results are induced by the lack of wall teichoic acids. *ΔdltA*, lacks D-alanylation and therefore a positive charge at the tip of the WTA or LTA polymer[25], whereas the *ΔltaS* strain does not synthesise LTA's[2]. *ΔtuaA* is not able synthesise teichuronic acids, a pathway suppressed in the phosphate rich medium LB[14].

In order to gain more insight in the *ΔtagO* conditional knock out strain, we monitored growth in LB medium and analysed matching microscopy pictures. The characterisation of the mutant regarding cell envelope and morphology is important, as these factors play a major role in e.g. cell division or lysis. In literature to date these features are not well described for *ΔtagO*[17]. Subsequently we elucidated the link between slow growth and aberrant morphologies. Cell shape is often referred to as a key feature of *ΔtagO* mutants[17], but not described in more detail. We here try to gain more insight into the cells morphology in different level of WTA expressions. As described in literature and in this report the *ΔtagO* mutant morphology is often referred to as spherical[2]. An in depth understanding of how the cell maintains a certain shape is not developed to date[37]. It is generally accepted that mechanical influences such as the already mentioned turgor pressure and cytoskeletal filaments play a role as well as the cell envelope.[38] With the apparent shape of the *tagO* deficient mutant (Figure 8), the question is raised what the influence of wall teichoic acids on the rigidity of the cell shape is. To examine this in more depth, microscopy pictures from the *ΔtagO* mutant without IPTG and samples supplied with 10 nM IPTG, 100 nM IPTG and 1000 nM IPTG respectively were compared to the WT. Morphology of the obtained strain is very similar to the cell wall less L-form of *Bacillus subtilis* created by Errington and Co-workers[39]. Therefore the PG content was matter of investigation as well. To reassure our results and link them directly to existence of WTA's, we examined length and occurrence of the polymer in mutants.

This knowledge is used to start analysing WTA influence on autolysins; here the regulation of ion homeostasis was examined, as it has been shown to be apparent in *Staphylococcus aureus*[17]. Binding capacity of Cytochrome C to *Bacillus subtilis* with WTA concentrations is used to depict their ability in cation binding.

Material and Methods

Strain description and growth

The liquid cultures of *Bacillus subtilis 168* and derivatives were grown in Lysogeny Broth medium (LB)(Table 3) at 37°C and 200-225 rpm shaking. When necessary the media was supplemented with 1mM isopropyl-BETA-D-thiogalactoside (IPTG), 5 µg ml^{-1} neomycin(neo) and/or 100 µg ml^{-1} spectinomycin(spec), when grown from a -80°C stock. *ΔtagO* is supplied with a spectinomycin resistance cassette, but has been grown without adding this antibiotic, as it led to better growth in the inoculation culture. The glycerol stocks for storage at -80°C were prepared by mixing 1 ml of liquid culture in logarithmic growth phase with 250µL of Glycerol 85%.

In all mutant strains used, the corresponding gene is conditionally knocked out. The gene is reintroduced into the *amyE* locus under the control of a P_{spank} promoter, which is inducible by IPTG. The strains used are shown in Table 1.

Table 1: Strains used including notation source and the necessary supplement for inoculation.

Strain	Characteristics	Source	Resistance
Bacillus subtilis 168	*dltA*::*neo*,*amyE*:Psp-*dltA*	Rik de Vries [40]	neo,spec
Bacillus subtilis 168	*ltaS*::*Neo*,*amyE*:Psp-*ltaS*	Rik de Vries [40]	neo,spec
Bacillus subtilis 168	*tuaA*::*Neo*,*amyE*:Psp-*tuaA*	Rik de Vries [40]	neo,spec
Bacillus subtilis 168	*tagO*::*Neo*,*amyE*:Psp-*tagO*	Rik de Vries [40]	neo,spec
Bacillus subtilis 168	WT	Maarten Mols[41]	-

Growth curves

For the growth curves, cells were inoculated into LB from -80°C stock overnight. The next day, cultures were washed once with preheated LB and diluted too an OD of 0.1 in 10mL LB and IPTG concentrations ranging from 0-1000 nM at 37°C and 200-225 rpm agitation. OD was measured hourly including blanking beforehand. Data was processed in windows office excel too give a line chart with a logarithmic scale of OD_{600} on the y-axis and the time in hours on the x-axis.

Growth was also monitored in the TecanGenios shaker: 200 µL LB was added per well plus 2 µL of corresponding IPTG concentration and 2 µL of bacteria solution from the overnight culture. Tecan was set to measure OD_{567} at 37°C every 10 minutes with a constant orbital shaking on the highest degree. Triplets of each sample were measured.

Again the data was processed in windows office excel. Average values of the triplet data set were calculated and subtracted of the average of all blank measurements, a triplet of 200 µL LB without additions. The graph was plotted in excel showing error bars indicating the highest and the lowest result respectively, to give a line chart with a logarithmic scale of OD_{600} as y-axis and the time in hours as a x-axis.

Sequencing

To sequence the P_{spank} promoter region it was amplified via Polymerase chain reaction (PCR).The strains were grown as described above in an overnight culture. The DNA was purified using the NucleoSpin® plasmid easy pure kit or the g-DNA kit respectively (Macherey-Nagel).

The PCR amplification was performed in a total volume of 50 µL: containing 10 µL Phusion polymerase buffer(Thermo scientific), 5 µL 2mM dNTP's, 31.75 µL MilliQ water, 1 µL AmyE forward primer, 1 µL AmyE reverse primer,1 µL sample DNA and 0.25 µL Phusion high-fidelity DNA Polymerase. Amplification took place using the following program: 30 seconds a 98°C, followed by 35 cycles of 10 seconds at 98 °C, 20 seconds at 57°C and 2 minutes 30 seconds at 72°C. After the cycles the samples were kept at 72°C for another 2 minutes and then stored at 4°C.

The product was purified using a NucleoSpin® Gel and PCR Clean-up kit (Macherey-Nagel). For correct DNA size-estimations and for isolation of DNA fragments, the DNA fragments were separated by agarose gel electrophoresis, stained with ethidium bromide and run along an appropriate DNA marker.

The obtained DNA was send for sequencing to Macrogen using the pDR110_RV as reverse primer and pDR110_RV as forward primer in *Bacillus subtilis* plus the Psp-TagO_FW as forward primer in *E.coli*.

Table 2: Primer used for sequencing.

Name	Sequence
AmyE forward primer	CGAGGGAAGCGTTCACAGTTTCG
AmyE reverse primer	CTTTCGGTAAGTCCCGTCTAGC
pDR110_FW	ACGCCAATCAGCAACGAC
pDR110_RV	GCTGCAGGAATTCGACTCTC
Psp-TagO_FW	AATACCGTCAGCGGATAAGC

Cytochrome C test

Cytochrome c is a small heme protein from eukaryotic cells[42]. Two features make it suitable for this test. First, it binds a cation, which can still build a chelate complex with e.g. a phosphate group in the cell envelope. The second is, that it has a distinct absorption at 526 nm wavelength[25]. Bacteria of the different strains were inoculated into LB from the -80°C stock and grown overnight. Then they were inoculated in 10mL LB and corresponding IPTG concentrations at 37°C and 200-225 rpm shaking and grown for 4 hours. The cells were collected by centrifugation at 7000 rpm for 10 min at room temperature (RT) and resuspended in 0.1 M HEPES buffer, pH 7.1, to OD 1.0 at 600nm. Cytochrome C was added to give a final concentration of 500 µg per ml. After incubation for 10 min at 37°C and 220 rpm shaking, the bacteria were removed by centrifugation (12000 rpm, 2 min, RT). Binding of cytochrome C was expressed as (ΔA_{526}) the difference between the absorbance of the initial concentration (A_{526i}) and the absorbance in the supernatant after pelleting the bacteria (A_{526s}) [25].

$\Delta A_{526} = A_{526i} - A_{526s}$

Microscopy and ImageJ

For visualisation of the different strains, microscopy was performed. Cells from different time points during growth curves were taken, centrifuged down at 14.000 rpm for three minutes, and re-suspended in 70% ethanol at -20°C for fixation. Fixed sampled were stored at -20°C for up to 10 days. The samples were again centrifuged (14.000 rpm, 3min) resuspended in water and air dried on a 1% agarose slide. Photos of slides were taken with Olympus IX71 inverted microscope with use of 100x phase contrast objective (Olympus 100X/1.40, Plan Apo, IX70), GFP FP filter and SoftWorx software. The following image properties were set: XY Dimensions: 1024 x 1024; ZWT Dimensions (expected): 1 x 2 x 1, Pixel Size: 0.06430 0.06430 0.200; Binning: 1x1. For visualising bright field the following settings were used: exposure time 0.05 seconds, EX filter: GFP-FITC, EM filter: GFP-FITC, ND filter: 32% or 50%. Microscopy pictures of the time point two hours after inoculation were analyzed with FiJi software [43]. For size analyses the scale was set to 15.492 pixels per µm. Cell area of 200 sample cells per strain was measured. The measurement has an area in μm^2 as a result, areas are assembled in different categories of size and the number in these categories is the input for the graph. The longest possible line inside the cell and an orthogonal line to measure length and width of the cell were also taken. The data was processed in windows office excel, by dividing width by the corresponding length, creating a ratio for each measured cell. For area and ratio data categories were defined, in which the frequency of the different sample was then calculated and occurrence

compared. To examine the influence of the apparent shape and ratio differences on the volume of a bacterium the averages of length as well as width for each sample are taken and a volume is calculated. For the WT a cylinder shape was used as approximation(Equation 1).

$$V = l * \pi r^2$$

Equation 1: Equation for volume of a cylinder. V:volume l: measured length of bacterial cell sample r: measured width divided by 2 as radius.

For the *ΔtagO* deletion strain samples, the better approximation is an ellipsoid is used(Equation 2). When r and l are the same length this equation becomes the equal to the one of a sphere.

$$V = \frac{4}{3} * \pi * r^2 * l$$

Equation 2: Equation for the volume of a ellipsoid. V:volume l: measured length of bacterial cell sample r: measured width divided by 2 as radius.

Polyacrylamide gel of Wall teichoic acids

WTA extraction

WTA's were isolated from a 30 ml culture of *Bacillus subtilis* in exponential growth phase. The cells were grown in LB for four hours at 37°C and growth was monitored by OD_{600} measurements. Then they were collected by centrifugation (2000 rpm, 10 min, RT). The created pellet was washed once with 30 ml of buffer 1(Table 3)(2000 rpm, 10 min, RT) and resuspended in 30 ml of buffer 2(Table 3). The samples were then placed in a boiling water bath for 1 h, followed by collection via centrifugation (10000 rpm, 10 min, RT) and re-suspended in 2ml of buffer 2. After transferring to a 2-ml microcentrifuge tube, and sedimentation (14000 rpm, 10 min, RT), the pellet was washed once with buffer 2, once with buffer 3(Table 3), and finally with buffer 1, always followed by a sedimentation step (14000 rpm, 10 min, RT). After the last wash, samples were treated with proteinase K buffer and incubated at 50°C for approximately 4h. Following digestion, samples were washed once with buffer 3 and then at least three times with distilled H2O to remove the SDS, always followed by sedimentation step (14000 rpm, 10 min, RT). Samples were thoroughly re-suspended in 1 ml of 0.1 M NaOH and shaken at room temperature at 200 rpm for 16-20h to hydrolyze WTA. Insoluble cell wall debris was removed by centrifugation (14000 rpm, 10 min, RT), and the supernatant containing the hydrolyzed WTA was directly analyzed by polyacrylamide gel electrophoresis. The protocol is taken from Meredith et al. (2008) with all changes made described here[44].

polyacrylamide gel electrophoresis and staining

WTA samples were loaded on a polyacrylamide gel consisting of: 36 % 29:1 acrylamide/bisacrrylamide, 25% 0.15M TrisHCl Buffer pH 8.8, 0.4mg/mL APS and 0.4 µl/ml TEMED in 0.2M Tris Borate Buffer (TBB) (Table 3). The gels were polymerized overnight or at least 6 hours at 4°C. Samples were mixed with 0.2 volumes of Tris-borate buffer containing 2.0 M sucrose to increase sample density. The portions per cavity were: 15 µl sample, 3 µl TBB Buffer including 2.0 M sucrose and 5 µl bromphenol blue (1 mg/ml) tracking dye. The protocol used is taken from Wolters and co-workers with the changes made described[45]. Electrophoresis was performed at 70 V until the tracking dye was 2 to 4 cm from the bottom of the gel.

For staining a 0.1% stock solution of 'stains all' (Table 3) in formamide was prepared and stored in the dark at 4°C. A working solution was created by diluting the stock solution 1:20 with the diluent 10% formamide, 25% isopropanol and 15mM Tris-HCl, pH8.8 in water. The gels were shaken for 24h at room temperature, then the staining solution was refreshed and shaken again for 24h. The staining protocol is taken from sigma-aldrich.com 85663 stains all protocol, all changes are mentioned above. The picture was taken on a BioRad Gel Doc EZ imager, white tray with trans illumination.

Gram staining

A thin layer of bacteria suspension was put on a glass slide, air dried and heat fixed. This smear was flooded with crystal violet [2.0g Crystal violet in 20.0ml Ethanol (95%)] for approximately 60 seconds. The slide was then covered with Gram's iodine [1.0g Iodine, 2.0g Potassium iodide in 300ml Distilled water] for about 180 seconds and carefully decolorized with 95% ethanol until thinnest parts of the smear are colourless.

After washing with MilliQ Water the sample was flooded with safranin [0.25g Safranin in 100ml Ethanol (95%)] for approximately 60 seconds and again washed with MilliQ Water, followed by air drying. The different strains and their colour have been checked under an optical microscope with 100x magnification. Adopted from Bartholomew et al[46].

Table 3: Buffer and working solutions

Buffer Description	Recipe
LB medium	for 1L; 10g bactotryptone, 5g yeast extract, 10g NaCl; pH-7.5 (adjusted with NaOH),
WTA assay buffer 1	[50 mM 2-(N-morpholino)ethanesulfonic acid (MES), pH 6.5] 9.76g per L
WTA assay buffer 2	(4% [wt/vol] sodium dodecyl sulfate [SDS], 50 mM MES; pH 6.5) 4g SDS in 1L
WTA assay buffer 3	(2% NaCl, 50 mM MES, pH 6.5) 2g NaCl in 1 L
WTA assay proteinase K buffer	(20mMTris-HCl [pH 8.0], 0.5% [wt/vol] SDS, and 20 µg of proteinase K in 1 ml) 2.4228 g Tris per L, 0.5 g SDS per L, Adjust pH to 8.0 with the appropriate volume of concentrated HCl. Bring final volume to 1 liter with deionized water.
TBB Buffer	0.2M tris base, 0.2M boric acid, 20mM EDTA
Stains all	Sigma Aldrich 85663 'Stains-all'

Results

Deletion strains growth characterisation

To characterise the deletion strains, growth behaviour in the rich medium LB was tested. The conditional knockout strains *ΔdltA, ΔltaS, ΔtuaA* and *ΔtagO* were compared to the wild type (WT) of *Bacillus subtilis 168*. Figure 5 shows the growth of all strains in LB over a time period of 9 hours, without any induction by IPTG and an hourly measurement of the optical density at 600 nm (OD_{600}). Growth of *ΔdltA* and *ΔltaS* is comparable to growth of the WT, which confirms results of other publications[25], [47]. After a short lag phase, a logarithmic growth phase of approximately 3 hours is entered. It is followed by a phase of slower increase, resulting in the beginning of the stationary phase. The growth reaches its maximum OD_{600} of approximately 3.3, 6-8 hours after inoculation. A similar curve is monitored for *ΔtuaA*, which also has been described previously[48]. The slightly longer lag phase here results in a delayed logarithmic growth, compared to the WT. The maximum OD_{600} observed is just below 3 and followed by a stationary phase similar to WT, *ΔdltA* and *ΔltaS*. The doubling time for these strains lies just above 1 hour in the first five hours of growth.

ΔtagO however is impaired in growth. It proliferates for about 5 hours, till an OD_{600} of 0.35 giving a doubling time of 2.766 hours. A maximum OD_{600} of around 0.45 was measured when grown for the later described polyacrylamide gel examination of WTA (data not shown), but never more. This phase is not followed by a stationary phase, but directly by lysis, resulting in an OD_{600} of 0.11 after 9 hours. These results confirm earlier studies on *tagO* depletion strains in LB[19].

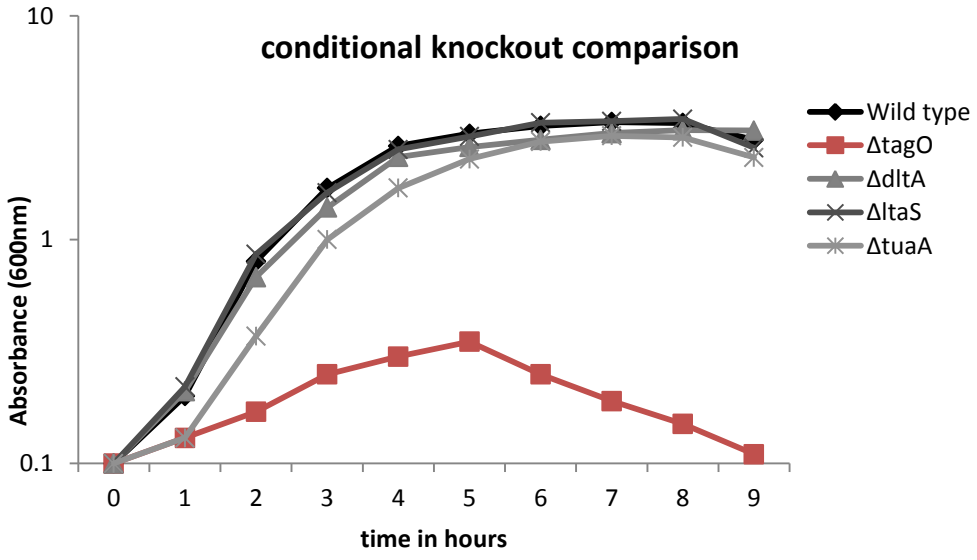

Figure 5: Representative growth curves of WT, *ΔdltA, ΔltaS, ΔtuaA* and *ΔtagO* strains in LB. Growth was measured hourly in optical density at 600 nm for 9 hours. The x-axis shows the time in hours, the y-axis the optical density in a logarithmic scale.

To gain further insight into the proliferation of the *ΔtagO* mutant, growth was monitored over a time period of 31 hours (Figure 6). The WT was compared to *ΔtagO* supplied with different IPTG concentrations reaching from no IPTG over 10 nM IPTG, 100 nM IPTG till 1000 nM IPTG. WT grows, as expected, to an OD_{600} of about 3.5 and stays around a value of 3 for the entire measurement. Measurements were taken hourly for the first 13 hours and again 25 and 31 hours after inoculation. Testing various concentrations of up to 10mM IPTG with *ΔtagO*, showed that 1000 nM IPTG was the maximum amount necessary for full possible complementation of the knocked out gene, concerning growth. Despite using high concentrations of IPTG, we were not able to fully complement growth of the *tagO* mutant(data not shown). As shown in Figure 6 the concentrations of 100 and 1000 nM IPTG already do not result in a significant difference to each other. For the first two hours they show a similar growth as the WT, leading to an OD_{600} of about 0.75 after 3 hours. This increase is severely slowed down in the next hour and followed by lysis to OD_{600} of 0.49. After 5 hours both samples start growing again reaching an OD_{600} of around 4 after 10-11 hours. This value is maintained till the end of the measurement.

The *ΔtagO* with 10 nM IPTG added reaches an OD_{600} of 0.5 after 3 hours., 2 hours of stationary phase is then followed by a decline to OD_{600} 0.3 till 8 hours after inoculation. The sample then grows again and stabilises well above OD_{600} 4 after 25 and 31 hours. The sample without IPTG shows similar behaviour as in Figure 5. After 3 hours a temporary maximum is shown at OD_{600} 0.38, followed by a steady decline to OD_{600} 0.1 after 13 hours. When measured after 25 and 31 hours however the sample showed an OD comparable to WT in stationary phase. The experiment has been repeated with addition of 20mM magnesium, as earlier studies indicate slower lysis and growth to higher OD when magnesium is present[25]. However, here no significant difference was observed (Data not shown).

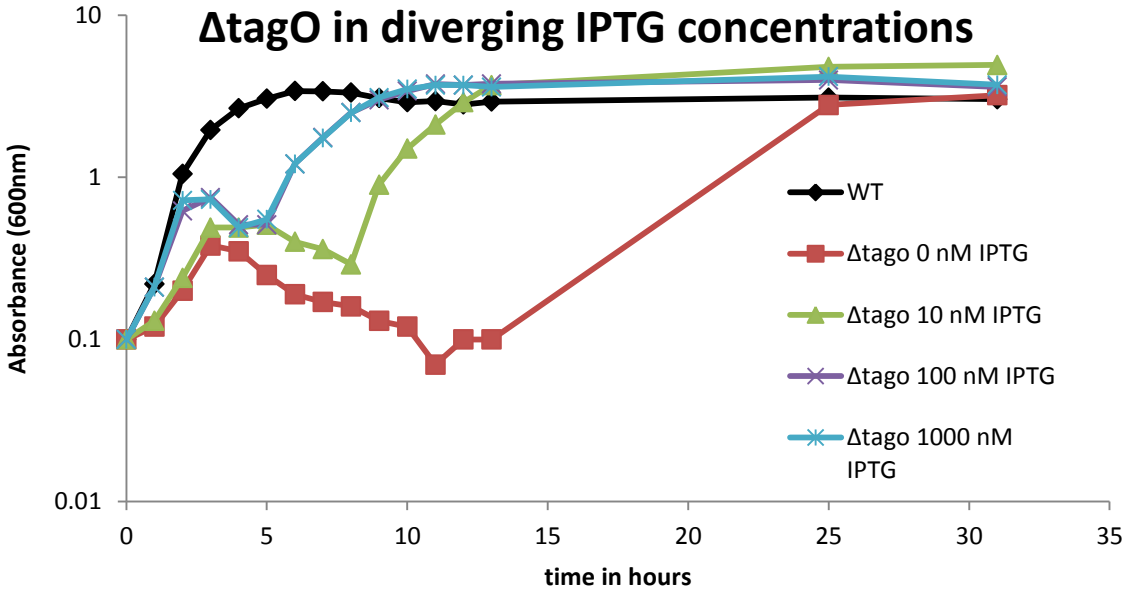

Figure 6: Representative growth curves of *ΔtagO* in presence of no, 10 nM, 100nM and 1000 nM IPTG compared to the WT. Hourly measurement of OD at 600 nm for 13 hours after that at 25 and 31 hours after inoculation. The x-axis shows the time in hours and the y-axis the OD in a logarithmic scale.

For further examination and to confirm the results shown above (Figure 6) the growth behaviour of *ΔtagO*, with the same IPTG concentrations added, was also tested for 17 hours in a Tecan Genios 96-well-plate shaker. Points show the average between the three samples for each concentration, the error bars indicate the highest and lowest single measurement at that exact time point.

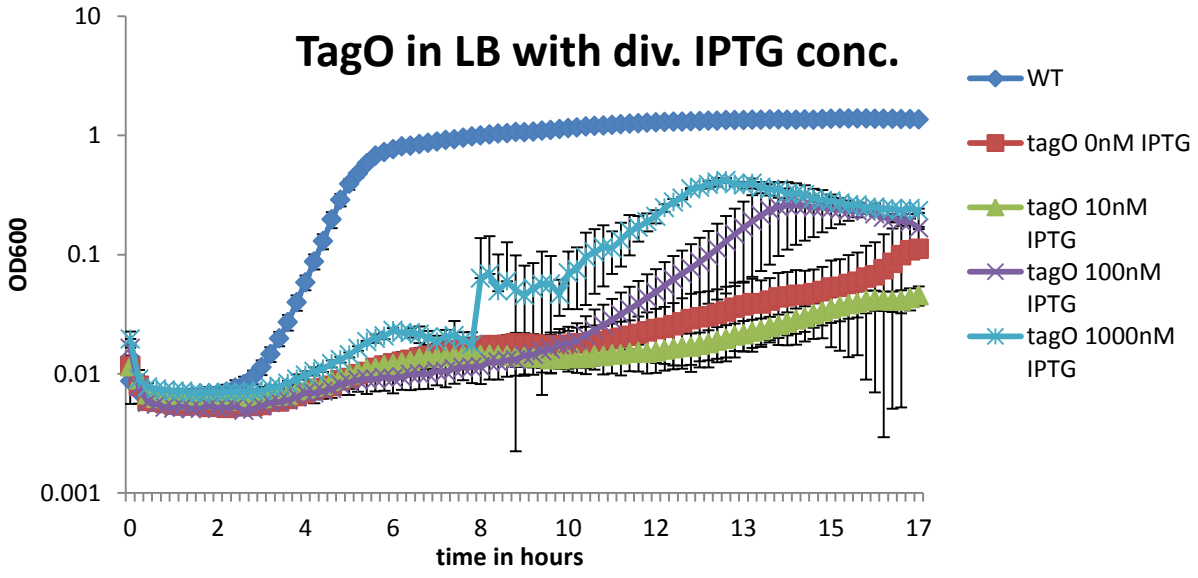

Figure 7: Tecan genios growth curves of *ΔtagO* in presence of no, 10 nM, 100nM and 1000 nM IPTG compared to the WT. Measurements were taken every 10 minutes for 17 hours . The average of a triplet measurement is shown, with the error bars indicating the highest and the lowest result respectively. The x-axis shows the time in hours and the y-axis the OD at 576 nm in a logarithmic scale.

The main difference in the result of the tecan experiment compared to the growth in Figure 6, is the lag phase that follows after a slight drop of OD_{576} in the very beginning of the measurement. After approximately two hours the WT starts to grow in a typical logarithmic fashion reaching the OD_{576} of around 1 after circa 5 hours 30 minutes (Figure 7). In general the strains used are growing slower compared to the wildtype than in the previous experiment. The samples with 100 nM IPTG present in the medium here grow slower than the ones without and with 10 nM IPTG added, for the first 8 hours. However it reaches a higher OD due to a faster growth after 8 hours. All strains again show a second lag phase, between 4 till 10 hours after inoculation. In contrast to the graph shown in Figure 6 significant lysis is not apparent. This could be connected to the much lower OD in the Tecan experiment compared to Figure 6, for the WT it has to be kept in mind that the Tecan reader is saturated at OD's higher than 1. None of the strains is able to grow to the OD 1 of the WT. Comparison between the two experiments is challenging, as the volume used is highly different and shaking might not be as sufficient in the 96-well plate to supply enough oxygen. Hence differences like the lag phase or the final OD are explainable. A similarity that is observable in both approaches and all samples, apart from the WT, is stagnation or even lysis followed by another growth phase. A second lag phase is unusual when the medium is not changed or interfered in any way. No change in pH, temperature or shaking procedure has been induced.

Microscopy pictures of every time point in Figure 6 were taken. Figure 8 shows time points of 1, 3, 7, 13 and 25 hours after inoculation for all samples.

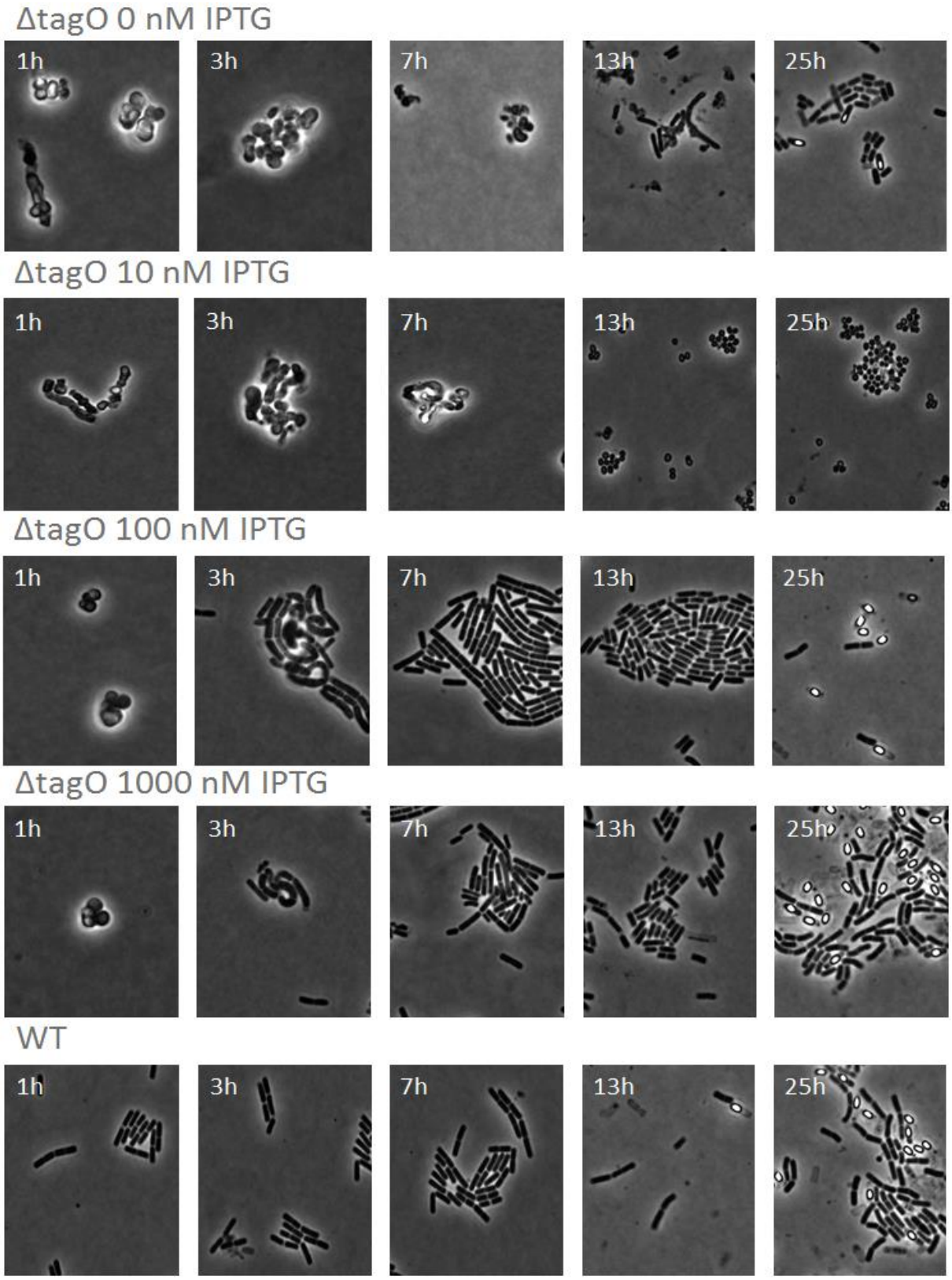

Figure 8: Microscopy pictures of the *tagO* mutant grown in LB with the different IPTG concentrations shown in Figure 6, the time points 1, 3, 7, 13 and 25 are selected as representative.

All strains, except the WT, show the typical and previously described *ΔtagO* spherical morphology 1 hour after inoculation[25]. In the sample not supplied with IPTG this morphology stays the same after 3 hours and lysis becomes visible in hour 7 and 13, corresponding to the graph in Figure 6. In fact the only viable cells after 13 hours already show a WT like rod shape. After 25 hours the morphology of the strain is similar to WT and starts to form spores. A spherical mutant has not been monitored to form spores. For the sample supplied with 10 nM IPTG a similar morphology is apparent after 5 hours, however a contamination starts to be visible and dominant from then on. Fast growth 8 hours after inoculation and the fact that the OD becomes significantly higher than the one of the WT can therefore be linked to this contamination. The samples with 100 and 1000 nM IPTG present show diverse morphology after 3 hours. Spherical and bulky rod shape cells are monitored, the cells do not grow during this period. After 7 hours both samples then are uniform in a rod shape appearance and remain like this, Figure 6 shows growth in this phase. Spore formation is coming up in the 25 hour sample.

Sequencing

To investigate if regrowth of the *ΔtagO* samples in Figure 6 and Figure 7 is connected to a mutation in the P_{spank} promoter, the promoter region was sequenced but showed no alteration in base pair sequence.

Gram staining

Errington et al. created a L-form of *Bacillus subtilis,* L-form is a term for a mutant that lacks the entire cell wall, including the PG[39]. As the spherical form of *ΔtagO* has a similar morphology the integrity of the cell envelope and specifically occurrence of PG was tested by Gram staining. The method only stains an intact cell envelope when PG is present and cross-linked.[46] The staining revealed that the PG network in *ΔtagO* is intact as the mutant was stained like the gram positive WT. Using a longer de-staining time showed that the stain stays longer in the mutant then in the WT, indicating the presence of a thicker cell wall.

Measurement of cell size

Cells for measurement were taken from cultures 2 hours after inoculation. As a first indication of diverging morphology the area of 200 cells per sample was measured using the imageJ software (

Figure 9). Full data is shown in the support data section (Appendix

Table 5). A narrow range in area size with a peak at 2.5 µm^2 and no cells with an area above 5.5 µm^2 is measured for the WT. The sample of 100 and 1000 nM IPTG supplement shows most occurrence between 5.5 and 6 µm^2 but a broader spectrum in size as the peak is less narrow and some cells show an area size of as much as 7 µm^2.

The area sizes of the samples with no or 10 nM IPTG added are broader spread with the highest occurrence between 3 and 3.5 µm^2 and also show a broad occurrence, but lower numbers in the larger area sizes of 7 and 7.5 µm^2.

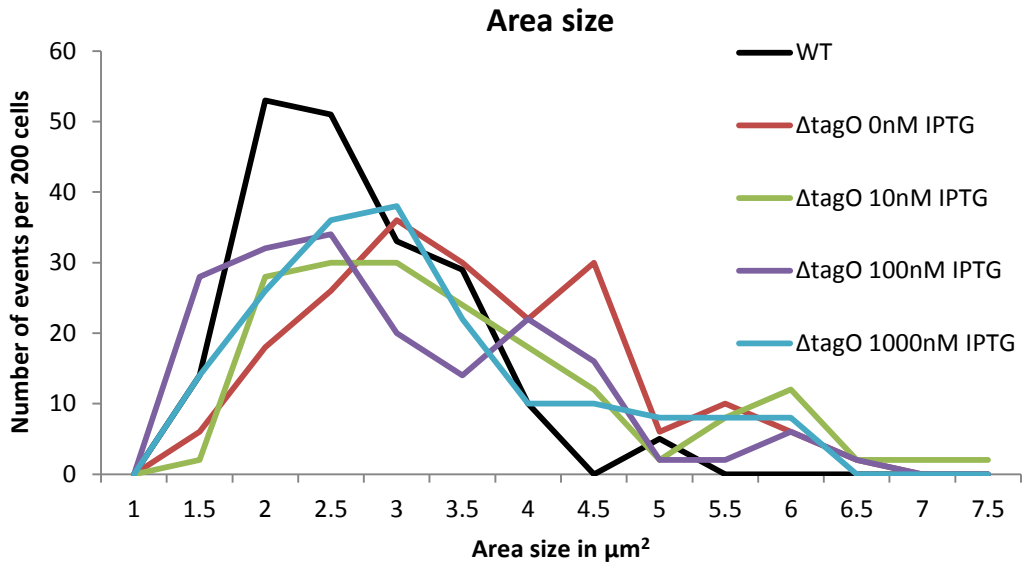

Figure 9: Cell area of WT and *ΔtagO* with no IPTG and with 10 nM, 100nM and 100nM IPTG added. Distribution of area is on shown x-axis and the frequency on the y-axis.

Area size indicates differences in size between the samples, but does not clarify if these are related to different shapes.

To analyse how round a cell is, the 200 cells per sample were also measured in the longest axis possible and orthogonal to this in the width. The width was then divided by the length to give a ratio pointing out how round or rod shape a cell is. A result of 1 stands for a perfectly round cell. Figure 10 shows a bar chart with categories, ratios are shown on the x-axis and the occurrence of the samples in them is indicated by the height on the y-axis. wild type shows a very distinct peak displaying only cases of ratios between 0.01 and 0.05. The samples with an addition of 100 and 1000 nM IPTG demonstrate ratios mainly between 0.1 and 0.4 and a broader distribution, which stands for a higher variety in cell morphology and a less distinct rod shape in the sample cells. A more ellipsoid then rod shape is displayed by the most events around 0.45 of the sample with 10 nM IPTG . This effect is

enhanced in the sample without IPTG. Here most occurrences are around 0.6 in ratio, clearly pointing towards an ellipsoid or even spherical shape.

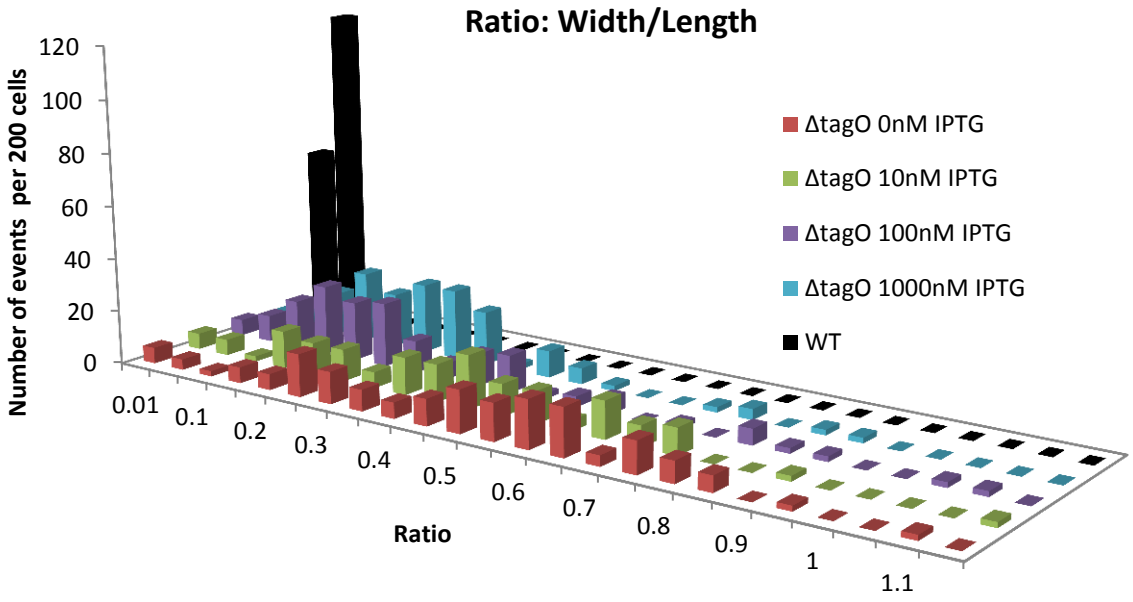

Figure 10: Distribution of the ratio calculated by dividing the width with the length. Distribution of ratios is shown on the x-axis, the frequency on the y axis.

The volumes calculated from the average length and width of the 200 cells per sample are shown in Figure 11. A difference in volume is apparent: with just over 0.4 µm^3 the wild type is monitored as the smallest sample. *ΔtagO* shows a decrease in size the more IPTG is given. With 1.33 µm^3, about 332.5% of the WT, the sample with no IPTG displays the biggest average cell volume. Adding 10 nM of IPTG leads to an average volume of 1.16 µm^3(290%), 100 nM IPTG to about 1 µm^3 (250%) and 1000 nM IPTG 0.75 µm^3(187.5%). Again the supplementation with IPTG is not able to complement the WT structure in the mutant fully.

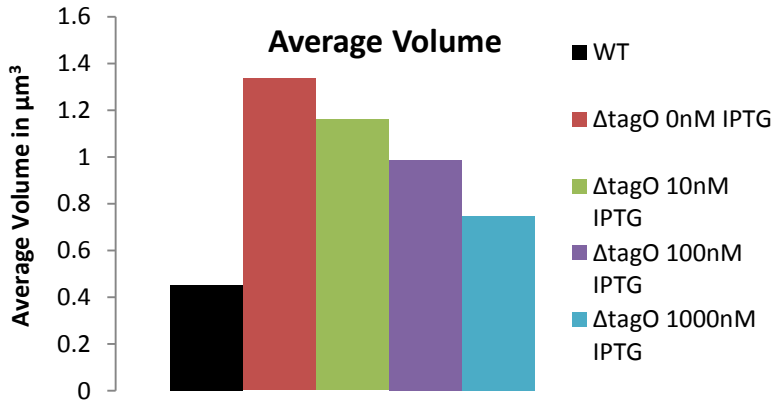

Figure 11: Average Volume in µm^3 of WT and *ΔtagO* with varying IPTG concentrations.

WTA assay

Deletion of the *tagO* gene should result in a mutant not able to synthesise wall teichoic acids[17]. The strain used here is a conditional knock out. This means the gene is reintegrated into the genome. It is under control of a regulated promoter, the P_{spank} promoter can be switched on by supplying IPTG. This system can be leaky, causing the occurrence of WTA's even without IPTG induction[49]. Existence, charge and length of the polymers built by the induced gene are tested. Therefore the wall teichoic acids have been extracted and different samples of *ΔtagO* were compared to WT on a polyacrylamide gel (10 nM and 100 nM IPTG plus the WT). Figure 12 shows a broad and thick band for the wild type, indicating a variety in length and a high concentration of wall teichoic acids. The bands in the lanes of the *ΔtagO* mutant with three different IPTG concentrations are significantly higher on the gel. This correlates to a greater length of the polymer. *ΔtagO* without induction shows only a very weak band, but indicates that even if no IPTG is given some wall teichoic acids are build. Bands get thicker and more visible, when more IPTG is added. (Lanes 3 and 4)

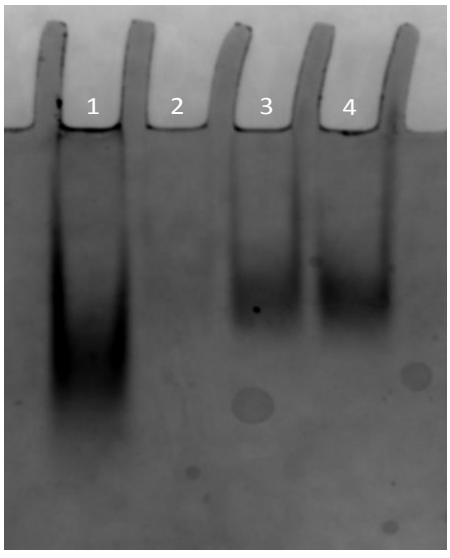

Figure 12: Polyacrilamide gel picture of WTA assay. 1) WT 2) *ΔtagO* no IPTG 3) *ΔtagO* 10 nMIPTG 4) *ΔtagO*100 nM IPTG

Cytochrome C test

As described earlier, wall teichoic acids have anion backbone and create a negatively charged environment in the cell envelope[12]. To test the charge distribution with and without WTA's present, a cation binding, cytochrome c test was conducted. In the first measurement (Table 4A) the mutants *ΔdltA, ΔltaS* and *ΔtuaA* were tested and compared to the WT. *ΔltaS* and *ΔtuaA* show a very similar cation binding capacity as the WT, *ΔdltA* however binds 119% of the WT capacity. This result was already obtained by Wecke et al.[25] and is reproduced here.

Table 4B shows the results for the *ΔtagO* mutant without IPTG and samples supplied with 10 nM IPTG, 100 nM IPTG and 1000 nM IPTG respectively. A 20% decrease in binding capacity in comparison to the WT, is monitored if no IPTG is given. In the sample with 10 nM IPTG a 23% decrease compared to the WT is observed. The capacity of 100 and 1000 nM IPTG is 11% below the one of the WT. These results show a direct correlation between the presence of wall teichoic acids in the cell wall and the cation binding capacity.

Strain	ΔAbsorbance	Comparison to WT in %
WT	0.155	
A)		
ΔdltA	0.183	+19%
ΔltaS	0.152	-1.6%
ΔtuaA	0.155	+/- 0%
B)		
***ΔtagO* 0 nM IPTG**	0.127	-20%
***ΔtagO* 10 nM IPTG**	0.122	-23%
***ΔtagO* 100 nM IPTG**	0.142	-11%
***ΔtagO* 1000 nM IPTG**	0.142	-11%

Table 4: A) ΔAbsorbance of the strains *ΔdltA, ΔltaS* and *ΔtuaA*, compared to WT in percent. **B)** *ΔtagO* with no, 10 nM, 100nM and 1000 nM IPTG added compared to WT in ΔAbsorbance.

Discussion

Deletion strains growth characterisation

The aim of this study was to investigate the influence of wall teichoic acids on *Bacillus subtilis 168* with a detailed view on cell shape and cation binding. At first growth behaviour of the strains *ΔdltA*, *ΔltaS*, *ΔtuaA* and *ΔtagO* was tested(Figure 5) and confirmed results in other studies[19], [25], [47], [48]. Complementation of the gene in the conditional knock out mutant *ΔtagO* was tested at different IPTG concentrations (Figure 6). This reactivation is not able to complement the WT like growth, a phenomena seen in all experiments conducted with the *ΔtagO* mutants strain and will be discussed in detail later.

As already mentioned in the result part a second growth phase after lysis as seen in Figure 6 is unusual. One reason for this could be changes in the pH of the medium, which affect the mutant more than the WT. Another explanation is the occurrence of a subpopulation in the -80°C stock of *ΔtagO*. This population might have mutated the lacI repressor or the P_{spank} promoter to not be functional anymore, giving the population the chance to grow as the WT but starting from a lower OD. Either the lacI repressor is not able to bind to the promoter and therefore not repress it, or the promoter itself is changed to not allow binding of lacI anymore.

A mutation in the promoter has been ruled out by sequencing, this still has to be done for the lacI. The repressor, with more than 1000 base pairs (bp), is more susceptible for mutations than the much smaller promoter (~35bp). The different time points of regrowth are an argument against a mutation in the stock culture, especially when both, the tecan (Figure 7) and the manual growth curve (Figure 6) are taken into consideration. A subpopulation would be the same size in all samples, as they are inoculated from the same overnight culture. Assuming a constant growth of this subpopulation , it would then be expected to be detectable at the same time in all samples within Figure 6 and Figure 7. This detectability holds true for the growth curves as well as the microscopy pictures. That these mutations appear in all samples but at different time points is unlikely, especially because the change in shape and growth behaviour in Figure 6 for the samples containing 100 and 1000 nM IPTG already occurs after three hours. If calculated back to the inoculation, this would indicate a subpopulation with an OD of about 0.001 initially mutating at the same time. This OD is estimated to contain $8*10^5$ Colony Forming Units (CFU) as the original OD of 0.1 is estimated to $8*10^7$ CFU per ml, ruling out the possibility of a single mutation being responsible for the change[50]. Additionally, the samples of 0, 100 and 1000 nM IPTG addition were kept as stock cultures and later regrown using antibiotics as described in material and methods, which shows that a WT contamination cannot be responsible for the late growth changes. Teichuronic acids could be responsible for regrowth and morphology

change back to the WT, as they fulfil similar functions under phosphate limited conditions[15], [16]. However, the medium used contains enough phosphate to suppress this pathway. To verify this, an assay similar to Figure 12 of the strains preserved from hour 31 in Figure 6 for teichuronic acids could be conducted. The occurring regrowth in these samples needs further study.

Figure 6 shows that a supplementation with IPTG of 100 or 1000 nM does not make a difference in growth. This indicates the highest feasible expression of the reintroduced gene at already 100 nM IPTG. The initial growth of no and 10 nM IPTG added is also similar, which suggests a corresponding expression of *tagO*. The area between 10 and 100 nM IPTG is therefore interesting to study further. The variety of *tagO* expression induced by concentrations between these values is most likely to produce diverging results. This can be used in comparison studies towards the influence of wall teichoic acids on cell features and behaviour.

Cell wall integrity

As mentioned earlier, the spherical shape of *ΔtagO* is similar to the cell wall depleted L-Form of *Bacillus subtilis* constructed by Errington and co-workers[39]. By Gram staining we can here show that the cell envelope is intact. However Gram staining is a straight forward but also hardly quantifiable technique[46]. The influence of wall teichoic acids on peptidoglycan synthesis is a highly discussed topic[17]. We suggest further studies with the mutant used in this report to gain more insight in the structural changes of PG with different level of wall teichoic acid expression. In 2008 Foster et al. published a detailed analysis of peptidoglycan structure in *Bacillus subtilis*[4]. To elucidate the *ΔtagO* PG structure we suggest a similar approach. The study concentrated on cell wall thickness, cross-linking between PG polymers and rigidity of the network.

Another approach would be detailed NMR investigation of cross linking as conducted by Schäfer et al. in 2006[51].

In our results concerning cell shape (Figure 9, Figure 10 and Figure 11) rigidity of the cell envelope is investigated. Jiang and co-workers (2011) show by a model, based on the free energy development, that a round cell, thermodynamically seen, is more favourable than a cylindrical rod shape.[38] This means the cell invests energy into maintaining the rod shape, especially during growth, as here nascent material is connected to old structures under the turgor pressure. This indicates that the cell needs structures preserving a rod shape. We showed via Gram staining, that the round *ΔtagO* still contains an intact and cross-linked PG layer. We also report an expansion in cell volume of up to 332% on average without teichoic acids compared to the WT, pointing out that the PG is not the part of the cell wall that provides rigidity. Studies for the Gram negative *E.coli* have shown an expansion of the PG layer till up to 300% of its relaxed state[52]. Our result shows this for gram positive

bacteria, where the PG network is much thicker and more dense than its gram negative counterpart. However our results are taken from fixed cells. It needs to be elucidated if viable cells show a different morphology, when measured in such detail.

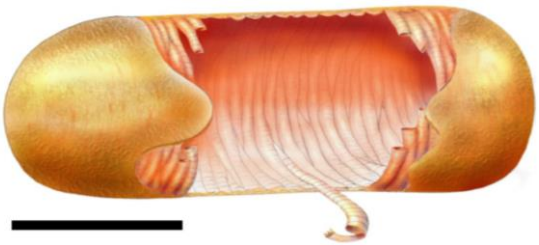

Figure 13: *Bacillus subtilis* cell wall model. Cable orientation with supercoiled substructure and cross striation of peptidoglycan is shown in cell wall cylinder.(bar for scale, 1 µm.) [53]

The PG strands are shown to have a natural right-handed twist[54], [55], completed strands and nascent material are arranged helically[53](Figure 13). *Bacillus subtillis* furthermore has a cross link index between 29% and 33%, which is lower than in gram negative bacteria[56], or *Staphylococcus aureus*[57]. In the cross linking peptide sequence starting from the MurNAc; L-alanine (Ala), D-glutamic acid (Glu), meso-diaminopimelic acid (A_2pm) and D-alanine occur. An additional characteristic for the *Bacillus subtilis* cell wall is the amidation of the free carboxylic group of A_2pm[58]. Amidation reduces the charge density in the walls, by neutralizing the acidic carboxyl groups. This influences the polyanionic network as it increases the importance of wall teichoic acids for supplying the negative charge, making *Bacillus subtilis* more susceptible when lacking them.

It has also been shown in *Staphylococcus aureus,* that wall teichoic acids are acting a spatial regulators during cross-linking in the PG synthesis[59]. This result is supported by the finding of Brown et al. in 2006, here they report areas of thickened cell wall in *ΔtagO* mutants of *Bacillus subtillis*[29]. These findings concerning cross-linking, spatial regulation and integrity of only the PG combined indicate why the PG network shows this high degree of flexibility when no WTA's are present.

Maintaining cell shape of bacteria is influenced by many factors, such as MreB or FtsZ, which are peptide structures occurring in the cytoplasm[60][61][62][63]. If missing, the corresponding cell is curved or irregularly bended and twisted[64]. Fluorescence microscopy of MreB shows a helical cable-like structure just underneath the cytoplasmic membrane [60]. Where and how exactly they interact with the cell envelope remains to be elucidated. This is important as our results raise the question if and how these inner cellular shape giving structures are interacting with the wall teichoic acids. An attachment of inner cytoplasmic factors with the cell envelope is needed to maintain cell

shape[38], as the turgor pressure pushes outside and only a rigid connection is able to maintain a non-spherical shape.

A connection between the dividing mechanism and wall teichoic acids is shown by Yamamoto et al. in 2008. The binding affinity of the DL-endopeptidase LytF to its substrate the PG is investigated with and without WTA's present. The N-terminal LysM domain of LytF binds better to the PG if no wall teichoic acids are present, showing a inhibiting influence by the teichoic acids. The authors speculate that this influence is governed by the aforementioned MreB, which would close the circle to cell shape maintaining structures[63]. This hypothesis has to be further studied in detail, and taking all known shape inducing factors into account.

The variety in cell shape found can be seen as an indicator for the role of WTA's in cell rigidity. Additional effects on the bacterium not only by direct linkage to the WTA's, but also through indirect changes, have to be further studied. It has, for example, been shown that a defect in cell wall formation can influence the chromosome morphologies[33]. As a rod shaped bacterium senses its middle to start division, a round bacterium may be inhibited in this mechanism. The distribution of wall teichoic acids however is consistent all over the cell envelope, indicating that they are not playing a role in the orientation of the cell[65].

Wall teichoic acids in *ΔtagO*

We were able to show that the IPTG induced production of wall teichoic acids in the knock out mutant *ΔtagO* leads to higher bands on a native polyacrylamide gel (Figure 12). The gel analysis also shows more distinct band in the mutant then in the wild type. A similar experiment has not been conducted for a conditional knock out strain of *ΔtagO*. The difference in band height on the gel could be connected to the following reasons. As we work with a native gel, the first possible explanation is that a more positive charge of the WT sample could lead to the faster migration through the gel. This seems unlikely as the polymer is built by distinct enzymes which cannot alter the structure. The occurrence of D-alanylation however, needs to be tested to rule out a stronger positive charge in the mutant samples. The second possibility is that a greater length in the mutant samples leads to slower migration. A combination of both can also not be ruled out.

Bacillus subtilis W23 is known to adapt its wall teichoic acids synthesis to stress conditions and diverging environments[66]. We propose a similar reaction here. A lack of cation binding could lead to the up-regulation of the genes in the tag pathway, as shown for *Staphylococcus aureus* in cation limited media[35]. *tagO* is organised in one operon, the two other operons contain *tagAB* and *tagDEF,* respectively[3]. All *tag* operons are under control of the σA factor, but only *tagAB* and *tagDEF* are additionally controlled by cell and environmental signals[67].

In the *ΔtagO* mutant a low amount of initial TagO products are available. We hypothesise that a determination of polymer length via balanced processing of all intermediates becomes uneven and results in longer polymers. As more enzymes are present to elongate fewer starting points, polymers grow faster and are therefore longer when being transported out of the cytoplasm. The low variance in length could also be explained by such a biased biosynthesis. A greater length is more likely to be achieved before the polymer is transported out of the cell. However, in the aforementioned publication of Peschel et al. (2012)[35] the up-regulation is not tested by investigating the length of the polymers, but by measuring the phosphor content of the cell wall. This means, the here observed longer length could also be present in cells with an up-regulation of the tag genes due to phosphor deficient medium.

Further studies are needed to clarify what a greater polymer length is linked to. One possibility is an up-regulation of the pathway due to e.g. phosphor limitations in the media. Another one is a limited availability of the TagO product. A third option would be that both effects play a role.

The impact of creating fewer but longer polymers on the density and function of the polyanionic network needs further investigation.

For a quantification of wall teichoic acids in the *tagO* deficient mutant the phosphor content in the cell wall needs to be measured as done by Neuhaus and Pollack (1994)[68]. The fact that we see a band in lane 2 of Figure 12: Polyacrilamide gel picture of WTA assay. 1) WT 2) *ΔtagO* no IPTG 3) *ΔtagO* 10 nMIPTG 4) *ΔtagO100* nM IPTGFigure 12 shows that the P_{spank} promoter is leaky. By quantifying the amount of WTA also in this sample we would be able to determine how leaky it is. In all obtained results this leakiness has to be considered as an influencing factor. Alongside of this, the amount of teichuronic acids also should be matter of investigations, as they could replace the WTA's. It is shown that a *ΔtuaA*,*ΔtagO* double KO mutant is not viable, indicating a role of teichuronic acids despite no lack of phosphor[19].

Influence on cation binding

One function of the polyanionic network is to bind cations to the cell wall. In Table 4 A we confirm observations made by Wecke et al. (1997)[25]. As expected the *ΔtuaA* mutant does not show altered cation binding, as in LB medium the teichuronic acid production should be repressed. We are also able to confirm that lipoteichoic acids are not involved in cation binding. Even though the polymer structure is similar to the wall teichoic acid one, the positioning in the cell wall is different. The D-alanylation has a negative impact on binding capacity, if not present binding is increased by 19%. This confirms the results of Wecke et al. and is in line with the structural knowledge, as no partly positively charged zwitterion is loaded on the polymer[25].

Table 4 B shows that the wall teichoic acids are responsible for cation binding. A complementation of the WT level by IPTG induction is again not achieved. We report a deficiency in cation binding of up to 23%. Similar results concerning the impact of wall teichoic acids on cation binding are reported for *Staphylococcus aureus*[35], [69]. Cation binding is an example of testing the anionic capacity of the polyanionic network. This capacity stands also for the ability to bind protons[35]. Proton binding in the Cell wall has impact on other factors in the cell envelope in *Staphylococcus aureus*, such as the pH, but not on the membrane potential[35]. After a 3-4 hour long growth in Figure 5 and Figure 6, the sample lacking IPTG shows an immediate decrease in OD, indicating lysis . This is also apparent in the pictures taken and shown in Figure 8. Lacking a stationary phase may be related to the cation binding of wall teichoic acids. As protein interaction such as autolysin activity, has been shown to be influenced by proton density around the cell wall in *Staphylococcus aureus*.[35]

Outlook

We report a detailed morphological analysis of the *tagO* deficient mutant, showing the influence of WTA's on the cell envelope (Figure 11). We also report an increased lysis in *ΔtagO* (Figure 5,Figure 6). To further investigate the connection of these results to the function of wall teichoic acid, we tested cation binding (Table 4). In *Staphylococcus aureus* cation binding has been connected to proton density in the cell envelope, which has been shown to be influencing the activity of the major autolysin AtlA[35]. This is believed to be triggered by a change in pH dependent on the density of protons present. Further investigation towards this mechanism in *Bacillus subtilis* would need a more detailed view on the autolysins present. In *Bacillus subtilis* 35 definite or probable genes were identified in the genome to code for autolysins. They are organised in 11 families on the basis of amino acid sequences[36]. 2 major autolysins (LytC and LytD) account for 95% of the activity in the cell[36]. This diversity is different to *Staphylococcus aureus*. The next step of connecting wall teichoic acid influence on these two enzymes would be first to test the difference in lysis in a *ΔtagO*, *ΔlytC* or *ΔlytD* double or, if possible, even triple knock out mutant. The results must be compared to a *ΔlytC* and *ΔlytD* knock out with wall teichoic acids present. To confirm the influence of proton density and pH on the autolysins their activity needs to be tested. This can be done using zymography as shown by Sekiguchi and co-workers (1995) on minor autolysins in *Bacillus subtilis*[70]. We are able to show that wall teichoic acids play a role in cell morphology and cation binding. Both topics need further studying to be understood in detail and connected to inner-cellular cell shape influencing proteins and autolysin activity respectively.

References

[1] T. J. Silhavy, D. Kahne, and S. Walker, “The bacterial cell envelope.,” *Cold Spring Harb. Perspect. Biol.*, vol. 2, no. 5, p. a000414, May 2010.

[2] J. G. Swoboda, J. Campbell, T. C. Meredith, and S. Walker, “Wall Teichoic Acid Function, Biosynthesis, and Inhibition Jonathan,” *Chembiochem*, vol. 11, no. 1, pp. 35–45, 2010.

[3] F. C. Neuhaus and J. Baddiley, “A continuum of anionic charge: structures and functions of D-alanyl-teichoic acids in gram-positive bacteria.,” *Microbiol. Mol. Biol. Rev.*, vol. 67, no. 4, pp. 686–723, Dec. 2003.

[4] W. Vollmer, D. Blanot, and M. a de Pedro, “Peptidoglycan structure and architecture.,” *FEMS Microbiol. Rev.*, vol. 32, no. 2, pp. 149–67, Mar. 2008.

[5] A.L. Sonenshein, J.A. Hoch, R. Losick, “Bacillus Subtilis and Other Gram positiv Bacteria: Biochemisttry, Physiology, and Molecular Genetics." *American Society for Microbiology* 1993

[6] C.R. Harwood “Bacillus” *SpringerLink Biotechnology Handbook,* Vol. 2, 1989

[7] S. a Beers, A. G. Buckland, R. S. Koduri, W. Cho, M. H. Gelb, and D. C. Wilton, “The antibacterial properties of secreted phospholipases A2: a major physiological role for the group IIA enzyme that depends on the very high pI of the enzyme to allow penetration of the bacterial cell wall.,” *J. Biol. Chem.*, vol. 277, no. 3, pp. 1788–93, Jan. 2002.

[8] W. Keck, “MINIREVIEW Peptidoglycan as a Barrier to Transenvelope Transport,” *J. Bacteriol.*, vol. 178, no. 19, pp. 5555–5562, 1996.

[9] R. J. Doyle and R. E. Marquis, “Elastic, flexible peptidoglycan and bacterial cell wall properties.,” *Trends Microbiol.*, vol. 2, no. 2, pp. 57–60, Feb. 1994.

[10] B. Y. D. C. Ellwood and P. Down, “The Wall Content and Composition of Bacillus subtilis var . niger Grown in a Chemostat,” *Biochem. J.*, pp. 367–373, 1970.

[11] S. Morath, S. von Aulock, and T. Hartung, “Structure/function relationships of lipoteichoic acids.,” *J. Endotoxin Res.*, vol. 11, no. 6, pp. 348–56, Jan. 2005.

[12] C. Weidenmaier and A. Peschel, “Teichoic acids and related cell-wall glycopolymers in Gram-positive physiology and host interactions.,” *Nat. Rev. Microbiol.*, vol. 6, no. 4, pp. 276–87, Apr. 2008.

[13] N. Kojima, Y. Araki, and E. Ito, “Structure of the Linkage Units Between Ribitol Teichoic Acids and Peptidoglycan,” *J. Bacteriol.*, vol. 161, no. 1, pp. 299–306, 1985.

[14] J. B. Ward, “Teichoic and teichuronic acids: biosynthesis, assembly, and location.,” *Microbiol. Rev.*, vol. 45, no. 2, pp. 211–43, Jun. 1981.

[15] M. Lahooti and C. R. Harwood, “Transcriptional analysis of the Bacillus subtilis teichuronic acid operon,” *Microbiology*, pp. 3409–3417, 1999.

[16] B. Soldo, V. Lazarevic, M. Pagni, and D. Karamata, “Teichuronic acid operon of Bacillus subtilis 168,” *Mol. Microbiol.*, vol. 31, no. 3, pp. 795–805, Feb. 1999.

[17] S. Brown, J. P. Santa Maria, and S. Walker, “Wall teichoic acids of gram-positive bacteria.,” *Annu. Rev. Microbiol.*, vol. 67, pp. 313–36, Jan. 2013.

[18] I. B. Y. Naumova, A. S. Shashkov, E. M. Tul, G. M. Streshinskaya, Y. I. Kozlova, N. V Potekhina, L. I. Evtushenko, and E. Stackebrandt, “Cell wall teichoic acids : structural diversity , species specificity in the genus Nocardiopsis , and chemotaxonomic perspective,” *FEMS Microbiol. Rev.*, vol. 25, pp. 269–283, 2001.

[19] B. Soldo, V. Lazarevic, and D. Karamata, “tagO is involved in the synthesis of all anionic cell-wall polymers in Bacillus subtilis 168.,” *Microbiology*, vol. 148, no. Pt 7, pp. 2079–87, Jul. 2002.

[20] C. Ginsberg, Y. Zhang, Y. Yuan, and S. Walker, “In Vitro Reconstitution of Two Essential Steps in Wall Teichoic Acid Biosynthesis,” *ACS Chem. Biol.*, vol. 1, no. 1, pp. 25–28, 2006.

[21] Y. S. Park, T. D. Sweitzer, J. E. Dixon, and C. Kent, “Expression, Purification, and Characterization of CTP:Glycerol-3-phosphate Cytidylyltransferase from,” *J. Biol. Chem.*, pp. 16648–16654, 1993.

[22] S. E. Allison, M. a D’Elia, S. Arar, M. a Monteiro, and E. D. Brown, “Studies of the genetics, function, and kinetic mechanism of TagE, the wall teichoic acid glycosyltransferase in Bacillus subtilis 168.,” *J. Biol. Chem.*, vol. 286, no. 27, pp. 23708–16, Jul. 2011.

[23] L. Chin, Theresa; Burger, Max M; Glaser, “Synthesis of Multiple of Teichoic Acids* IV. The Formation of Multiple Wall Polymers in Bacillus subtilis W-23,” *Arch. Biochem. Biophys.*, vol. 116, pp. 358–367, 1966.

[24] J. J. May, R. Finking, F. Wiegeshoff, T. T. Weber, N. Bandur, U. Koert, and M. a Marahiel, “Inhibition of the D-alanine:D-alanyl carrier protein ligase from Bacillus subtilis increases the bacterium’s susceptibility to antibiotics that target the cell wall.,” *FEBS J.*, vol. 272, no. 12, pp. 2993–3003, Jun. 2005.

[25] J. Wecke, W. Fischer, and K. Madela, “The absence of D-alanine from lipoteichoic acid and wall teichoic acid alters surface charge, enhances autolysis and increases susceptibility to rnethicillin in,” *Microbiology*, vol. 143, pp. 2953–2960, 1997.

[26] K. Schirner, L. K. Stone, and S. Walker, “ABC transporters required for export of wall teichoic acids do not discriminate between different main chain polymers,” *ACS Chem. Biol.*, vol. 6, no. 5, pp. 407–412, 2012.

[27] V. Lazarevic and D. Karamata, “The tagGH operon of Bacillus subtilis 168 encodes a two-component ABC transporter involved in the metabolism of two wall teichoic acids,” *Mol. Microbiol.*, vol. 16, pp. 345–355, 1995.

[28] Y. Kawai, J. Marles-Wright, R. M. Cleverley, R. Emmins, S. Ishikawa, M. Kuwano, N. Heinz, N. K. Bui, C. N. Hoyland, N. Ogasawara, R. J. Lewis, W. Vollmer, R. a Daniel, and J. Errington, “A widespread family of bacterial cell wall assembly proteins.,” *EMBO J.*, vol. 30, no. 24, pp. 4931–41, Dec. 2011.

[29] M. a D'Elia, K. E. Millar, T. J. Beveridge, and E. D. Brown, "Wall teichoic acid polymers are dispensable for cell viability in Bacillus subtilis.," *J. Bacteriol.*, vol. 188, no. 23, pp. 8313–6, Dec. 2006.

[30] D. V Debabov, M. Y. Kiriukhin, and F. C. Neuhaus, "Biosynthesis of Lipoteichoic Acid in Lactobacillus rhamnosus : Role of DltD in D -Alanylation," vol. 182, no. 10, pp. 2855–2864, 2000.

[31] R. Biswas, R. E. Martinez, N. Göhring, M. Schlag, M. Josten, G. Xia, F. Hegler, C. Gekeler, A.-K. Gleske, F. Götz, H.-G. Sahl, A. Kappler, and A. Peschel, "Proton-binding capacity of Staphylococcus aureus wall teichoic acid and its role in controlling autolysin activity.," *PLoS One*, vol. 7, no. 7, p. e41415, Jan. 2012.

[32] T. Kern, M. Giffard, S. Hediger, A. Amoroso, C. Giustini, N. K. Bui, B. Joris, C. Bougault, W. Vollmer, and J.-P. Simorre, "Dynamics characterization of fully hydrated bacterial cell walls by solid-state NMR: evidence for cooperative binding of metal ions.," *J. Am. Chem. Soc.*, vol. 132, no. 31, pp. 10911–9, Aug. 2010.

[33] M. Elbaz and S. Ben-Yehuda, "The metabolic enzyme ManA reveals a link between cell wall integrity and chromosome morphology.," *PLoS Genet.*, vol. 6, no. 9, p. e1001119, Sep. 2010.

[34] R. M. Cole, T. J. Popkin, R. J. Boylan, and N. H. Mendelson, "Ultrastructure of a Temperature-Sensitive Rod- Mutant of Bacillus subtilis," *J. Bacteriol.*, vol. 103, no. 3, pp. 793–810, 1970.

[35] R. Biswas, R. E. Martinez, N. Göhring, M. Schlag, M. Josten, G. Xia, F. Hegler, C. Gekeler, A. K. Gleske, F. Götz, H. G. Sahl, A. Kappler, and A. Peschel, "Proton-binding capacity of staphylococcus aureus wall teichoic acid and its role in controlling autolysin activity," *PLoS One*, vol. 7, no. 7, p. e41415, Jan. 2012.

[36] T. J. Smith, S. A. Blackman, and S. J. Foster, "Autolysins of Bacillus subtilis : multiple enzymes with multiple functions," *Microbiology*, vol. 146, pp. 249–262, 2000.

[37] M. T. Cabeen and C. Jacobs-Wagner, "Bacterial cell shape.," *Nat. Rev. Microbiol.*, vol. 3, no. 8, pp. 601–10, Aug. 2005.

[38] H. Jiang, F. Si, W. Margolin, and S. X. Sun, "Mechanical control of bacterial cell shape.," *Biophys. J.*, vol. 101, no. 2, pp. 327–35, Jul. 2011.

[39] M. Leaver, P. Domínguez-Cuevas, J. M. Coxhead, R. a Daniel, and J. Errington, "Life without a wall or division machine in Bacillus subtilis.," *Nature*, vol. 457, no. 7231, pp. 849–53, Feb. 2009.

[40] H. J. De Vries, "Surface behavior of cell-wall altered Bacillus subtilis 168," 2012.

[41] V. Barbe, S. Cruveiller, F. Kunst, P. Lenoble, G. Meurice, A. Sekowska, D. Vallenet, T. Wang, I. Moszer, C. Médigue, and A. Danchin, "From a consortium sequence to a unified sequence: the Bacillus subtilis 168 reference genome a decade later.," *Microbiology*, vol. 155, no. Pt 6, pp. 1758–75, Jun. 2009.

[42] M. Tafani, N. O. Karpinich, K. a Hurster, J. G. Pastorino, T. Schneider, M. a Russo, and J. L. Farber, "Cytochrome c release upon Fas receptor activation depends on translocation of full-

length bid and the induction of the mitochondrial permeability transition.," *J. Biol. Chem.*, vol. 277, no. 12, pp. 10073–82, Mar. 2002.

[43] C. a Schneider, W. S. Rasband, and K. W. Eliceiri, "NIH Image to ImageJ: 25 years of image analysis," *Nat. Methods*, vol. 9, no. 7, pp. 671–675, Jun. 2012.

[44] T. C. Meredith, J. G. Swoboda, and S. Walker, "Late-stage polyribitol phosphate wall teichoic acid biosynthesis in Staphylococcus aureus.," *J. Bacteriol.*, vol. 190, no. 8, pp. 3046–56, Apr. 2008.

[45] P. J. Wolters, K. M. Hildebrandt, J. P. Dickie, and J. S. Anderson, "Polymer length of teichuronic acid released from cell walls of Micrococcus luteus.," *J. Bacteriol.*, vol. 172, no. 9, pp. 5154–9, Sep. 1990.

[46] J. W. Bartholomew and T. O. D. Mittwer, "THE GRAM STAIN," pp. 1–29, 19AD.

[47] K. Schirner, J. Marles-Wright, R. J. Lewis, and J. Errington, "Distinct and essential morphogenic functions for wall- and lipo-teichoic acids in Bacillus subtilis.," *EMBO J.*, vol. 28, no. 7, pp. 830–42, Apr. 2009.

[48] A. Bhavsar, L. Erdman, J. W. Schertzer, and E. D. Brown, "Teichoic acid is an essential polymer in Bacillus subtilis that is functionally distinct from teichuronic acid," *J. Bacteriol.*, vol. 186, no. 23, pp. 7865–7873, 2004.

[49] L. Vavrová, K. Muchová, and I. Barák, "Comparison of different Bacillus subtilis expression systems.," *Res. Microbiol.*, vol. 161, no. 9, pp. 791–7, Nov. 2010.

[50] D. Ghribi and S. Ellouze-Chaabouni, "Enhancement of Bacillus subtilis Lipopeptide Biosurfactants Production through Optimization of Medium Composition and Adequate Control of Aeration.," *Biotechnol. Res. Int.*, vol. 2011, p. 653654, Jan. 2011.

[51] L. Cegelski, D. Steuber, A. K. Mehta, D. W. Kulp, P. H. Axelsen, and J. Schaefer, "Conformational and quantitative characterization of oritavancin-peptidoglycan complexes in whole cells of Staphylococcus aureus by in vivo 13C and 15N labeling.," *J. Mol. Biol.*, vol. 357, no. 4, pp. 1253–62, Apr. 2006.

[52] A. L. Koch and S. Woeste, "Elasticity of the Sacculus of Escherichia coli," *J. Bacteriol.*, vol. 174, no. 14, pp. 4811–4819, 1992.

[53] E. J. Hayhurst, L. Kailas, J. K. Hobbs, and S. J. Foster, "Cell wall peptidoglycan architecture in Bacillus subtilis.," *Proc. Natl. Acad. Sci. U. S. A.*, vol. 105, no. 38, pp. 14603–8, Sep. 2008.

[54] S. O. Meroueh, K. Z. Bencze, D. Hesek, M. Lee, J. F. Fisher, T. L. Stemmler, and S. Mobashery, "Three-dimensional structure of the bacterial cell wall peptidoglycan.," *Proc. Natl. Acad. Sci. U. S. A.*, vol. 103, no. 12, pp. 4404–9, Mar. 2006.

[55] B. Leps, H. Labischinski, and H. Bradaczek, "Conformational behavior of the polysaccharide backbone of murein.," *Biopolymers*, vol. 26, no. 8, pp. 1391–406, Aug. 1987.

[56] J. Sekiguchi and H. Yamamoto, *4-3. Cell wall structure of*, vol. 661, no. 2. 2012, pp. 115–148.

[57] L. Y. Gal and A. Ronald, “Cell wall assembly in Staphylococcus aureus : proposed absence of secondary crosslinking reactions,” pp. 1907–1913, 1993.

[58] A. Atrih, G. Bacher, G. Allmaier, P. Williamson, S. J. Foster, N. Allmaier, and M. P. Williamson, “Analysis of Peptidoglycan Structure from Vegetative Cells of Bacillus subtilis 168 and Role of PBP 5 in Peptidoglycan Maturation Analysis of Peptidoglycan Structure from Vegetative Cells of Bacillus subtilis 168 and Role of PBP 5 in Peptidoglycan Maturati,” *J. Bacteriol.*, vol. 181, pp. 3956–3966, 1999.

[59] M. L. Atilano, P. M. Pereira, J. Yates, P. Reed, H. Veiga, M. G. Pinho, and S. R. Filipe, “Teichoic acids are temporal and spatial regulators of peptidoglycan cross-linking in Staphylococcus aureus.,” *Proc. Natl. Acad. Sci. U. S. A.*, vol. 107, no. 44, pp. 18991–6, Nov. 2010.

[60] L. J. F. Jones, R. Carballido-Lopez, and J. Errington, “Control of Cell Shape in Bacteria : Helical , Actin-like Filaments in Bacillus subtilis,” *Cell*, vol. 104, pp. 913–922, 2001.

[61] H. J. Defeu Soufo and P. L. Graumann, “Dynamic movement of actin-like proteins within bacterial cells.,” *EMBO Rep.*, vol. 5, no. 8, pp. 789–94, Aug. 2004.

[62] J. Errington and R. Carbadillo-Lopez, “The Bacterial Cytoskeleton : In Vivo Dynamics of the Actin-like Protein Mbl of Bacillus subtilis,” *Dev. Cell*, vol. 4, pp. 19–28, 2003.

[63] H. Yamamoto, Y. Miyake, M. Hisaoka, S.-I. Kurosawa, and J. Sekiguchi, “The major and minor wall teichoic acids prevent the sidewall localization of vegetative DL-endopeptidase LytF in Bacillus subtilis.,” *Mol. Microbiol.*, vol. 70, no. 2, pp. 297–310, Oct. 2008.

[64] G. C. Stewart and Y. Abhayawardhane, “Bacillus subtilis Possesses a Second Determinant with Extensive Sequence Similarity to the Escherichia coli mreB Morphogene,” *J. Bacteriol.*, vol. 177, no. 3, pp. 765–773, 1995.

[65] R. J. Doyle, M. L. Mcdannel, J. R. Helman, and U. N. Streips, “Distribution of Teichoic Acid in the Cell Wall of Bacillus subtilis,” *J. Bacteriol.*, vol. 122, no. 1, pp. 152–158, 1975.

[66] K. Minnig, V. Lazarevic, B. Soldo, and C. Mauël, “Analysis of teichoic acid biosynthesis regulation reveals that the extracytoplasmic function sigma factor sigmaM is induced by phosphate depletion in Bacillus subtilis W23.,” *Microbiology*, vol. 151, no. Pt 9, pp. 3041–9, Sep. 2005.

[67] C. Mauel, A. Bauduret, C. Chervet, S. Beggah, and D. Karamata, “In Bacillus subtilis 168, teichoic acid of the cross-wall may be different from that of the cylinder: a hypothesis based on transcription analysis of tag genes,” *Microbiology*, vol. 141, pp. 2379–2389, 1995.

[68] J. H. Pollack and F. C. Neuhaus, “Changes in wall teichoic acid during the rod-sphere transition of Bacillus subtilis 168.,” *J. Bacteriol.*, vol. 176, no. 23, pp. 7252–9, Dec. 1994.

[69] T. C. Ghosh, J. K. Ghosh, and M. K. Pal, “Studies on the Conformation of and Metal Ion Binding by Teichoic Acid of Staphylococcus aureus,” *Biopolymers*, vol. 30, pp. 273–277, 1990.

[70] M. H. Rashid, N. Sato, and J. Sekiguchi, “Analysis of the minor autolysins of Bacillus subtilis during vegetative growth by zymography,” *FEMS Microbiol. Lett.*, vol. 32, no. 95, 1995.

Acknowledgments

I would like to thank Marielle, for being helpful when help was needed, but also for granting me a lot of freedom and trusting me in my research. My thanks also go to Maike, who was always open for a question and full of advice. Dankeschön. I have to thank Oscar for many things; despite his very busy schedule he maintained an open ear for the project and for other questions. Especially with his letter of recommendation he helped me with my future plans My thanks go to the group of Molgen in general, as this big group manages to have a very nice working atmosphere and every single person a lovely and easy attitude towards new members. I think especially in this size it is something special and worth aiming for in future.

In a non-academic way I always have to thank my family and my girlfriend Johanna, without them my stress level would be a lot higher. But also talks and sports with Dimitra and Robin kept me sane and made my project more of a joy.

Appendix

Table 5: Supplemental data of imageJ measurement.

Area(μm^2)					Width(μm)					Length(μm)				
WT	0 nM IPTG	10 nM IPTG	100 nM IPTG	1000 nM IPTG	WT	0 nM IPTG	10 nM IPTG	100 nM IPTG	1000 nM IPTG	WT	0 nM IPTG	10 nM IPTG	100 nM IPTG	1000 nM IPTG
27.67	12.17	5.83	5.42	6.42	0.695	33.79	20.39	10.84	11.06	3411	34.11	27.44	37.01	27.21
33.08	12.25	7.33	8.21	8	0.73	31.8	22.03	10.55	11.8	3952	39.52	28.06	33.82	21.9
30.37	13.25	7.67	8.67	8.33	1.095	26.23	12.31	10.33	8.88	3589	35.89	52.54	36.13	25.81
21.25	14.46	11.04	9.37	11.5	0.645	13.82	11.95	10.55	8.4	2453	24.53	24.49	29.16	25.03
19.29	15.71	12.42	9.92	12.33	1.111	26.54	20.52	7.78	15.64	2614	26.14	58.43	32.51	18.24
32.17	15.96	15.12	10.33	12.37	1.033	31.49	43.02	16.48	16.99	2969	29.69	57.19	25.67	17.33
35.67	16.17	16.87	10.83	12.58	0.645	33.88	23.82	10.71	8.88	2843	28.43	38.59	37.59	14.6
24.92	16.25	17.5	10.87	13.25	1.033	17.42	23.87	9.61	11.06	2972	29.72	22.23	28.17	19.59
19.67	17.29	18.25	11.67	13.79	0.824	14.64	14.12	14.08	6.8	1959	19.59	18.72	22.9	31.38
15.21	18	18.33	11.75	14.75	0.528	19.27	12.2	14.04	7.78	1648	16.48	26.13	29.77	25.28
27.96	18.17	18.42	11.79	14.83	0.577	27.25	16.17	7.42	5.53	3874	38.74	28.31	49.07	26.19
36.58	18.79	18.46	12	15.5	0.921	26.07	23.51	13.31	6.64	3742	37.42	67.19	22.5	42.19
33.87	18.96	18.58	12	15.92	0.86	14.25	16.42	11.8	6.8	3558	35.58	36.98	41.19	31.2
31.62	19.17	18.58	13	17.33	0.737	18.36	8.57	22.27	5.83	3210	32.1	19.99	38.98	23.21
33.75	21	19	13.58	17.33	0.577	26.79	10.67	9.92	9.92	4011	40.11	30.85	50.46	22.39
20.5	21.08	19.04	14.21	17.37	0.742	22.85	17.42	11.8	7.6	2555	25.55	26.13	31.55	22.9
17.83	21.21	19.42	14.33	17.5	0.659	22.98	15.14	10.06	5.94	1815	18.15	30.21	22.9	21.77
15.71	21.29	19.75	14.37	17.62	0.659	19.54	9.03	16.69	7.37	1568	15.68	38.66	22.9	19.4
29.75	21.37	19.75	14.96	17.67	0.664	23.15	28.92	19.29	5.94	3650	36.5	69.01	23.6	27.7
32.37	21.58	19.83	14.96	18.04	1.1	14.9	14.69	8.9	9.21	3545	35.45	35.91	29.81	27.64
32.96	21.67	20.33	15.08	18.12	0.94	25.55	10.33	8.41	7.42	3224	32.24	18.43	26.16	25.6
24.58	22.75	20.54	15.21	18.17	1.006	22.54	16.48	7.58	9.65	2703	27.03	20.8	18.72	28.95
23.62	23.29	20.67	15.25	18.25	0.664	31.81	14.39	7.15	10.06	2977	29.77	24.35	28.91	43.71
27.5	24	21.08	15.29	18.87	0.816	26.8	19.22	8.37	5.21	2951	29.51	58.28	25.79	19.12
16.08	24.04	21.54	15.33	19.67	0.664	30.47	13.52	6.04	7.37	2424	24.24	33.64	23.45	21.19
23.83	24.33	21.62	15.79	20.04	0.553	25.79	19.95	6.54	5.53	2972	29.72	32.06	21.13	38.63
20.12	24.83	21.71	16.04	20.46	0.583	27.16	22.42	7.15	12.55	2740	27.4	40.72	20.38	17.46
24.96	24.92	21.87	16.29	20.54	0.782	25.55	18.24	6.37	7.46	3185	31.85	40.28	42.68	14.86
15.75	25.17	21.96	17.33	20.67	0.369	22.16	21.63	9.54	8.6	2280	22.8	27.11	14.97	14.39
14.58	25.54	22.33	17.87	20.92	0.412	19.76	14.86	7.72	20.93	2637	26.37	18.97	26.47	27.64

13.83	25.58	22.92	17.92	21.08	0.412	27.74	14.23	7.2	19.54	2424	24.24	25.39	19.97	23.5
12.79	26.21	23.04	18	21.67	0.659	21.6	24.73	6.9	11.84	1896	18.96	43.69	49.28	12.99
15.12	26.5	23.37	18.12	22	0.521	18.98	21.76	6.37	16.95	2075	20.75	31.55	22.24	20.43
21.79	26.71	23.75	18.67	22.58	0.664	14.64	25.11	6.37	18.72	2111	21.11	27.82	32.57	20.93
18.42	26.83	23.96	18.87	22.62	0.577	30.71	13.93	5.62	10.22	2639	26.39	28.8	21.97	22.1
14.79	26.96	24.04	19.5	22.96	0.664	11.39	16.93	9.25	12.56	2149	21.49	25.24	36.61	18.42
34.33	27.46	25.58	19.83	23.04	0.921	16.76	7.72	6.37	9.54	3578	35.78	15.88	15.37	33.9
18.37	27.46	26.33	20.04	23.04	0.778	23.35	9.05	7.72	8.29	1843	18.43	14.25	17.07	44.37
29	27.46	26.38	20.75	23.67	0.644	21.6	7.15	10.04	8.37	2949	29.49	7.72	41.85	21.34
12.5	27.58	26.46	20.87	23.75	0.84	18.81	20.16	9.21	9.76	1650	16.5	26.8	34.48	17.26
15.96	28.08	26.67	21.67	24.25	0.824	22.54	12.56	9.21	11.39	1731	17.31	16.57	36.98	19.9
36.04	28.12	26.75	21.92	24.33	0.709	30.32	18.81	17.89	7.58	4046	40.46	22.11	17.07	22.16
29.17	28.58	26.83	21.96	24.46	0.68	39.7	10.65	13.08	12.75	3957	39.57	17.76	13.08	12.75
24.62	28.62	27.08	22.21	24.5	0.742	22.62	11.39	16.85	10.18	3462	34.62	14.21	18.03	31.52
16.58	29.21	28.42	22.5	26	0.664	29.31	16.68	7.9	14.33	2560	25.6	14.03	10.91	42.15
19.46	29.21	28.54	23.08	26	0.715	17.76	11.23	13.23	9.05	2012	20.12	19.09	13.08	40.19
16.87	29.67	28.62	23.67	26	0.637	16.85	11.9	9.47	8.9	2171	21.71	17.97	11.66	26.96
19.62	30.08	28.87	23.75	26.12	0.609	24.79	10.59	6.37	5.92	2254	22.54	18.88	10.35	25.79
17.79	30.33	29	23.79	26.17	0.562	25.85	10.59	7.2	5.62	2397	23.97	12.99	28.57	30.33
26.29	30.5	29.12	23.79	26.33	0.71	25.13	13.08	5.86	11.39	2262	22.62	21.34	20.11	29.28
14.87	30.71	29.46	24.04	26.54	0.772	25.55	10.91	8.62	8.24	2416	24.16	24.1	39.23	28.47
16.08	30.92	29.58	24.17	26.75	0.89	16.74	10.49	9.54	9.02	1927	19.27	16.51	33.9	41.15
28.12	30.96	30.17	24.25	26.87	0.749	18.43	17.26	9.47	5.92	2997	29.97	23.03	40.53	55.49
29.96	31.46	30.29	24.25	27.12	0.675	23.5	10.65	6.54	8.29	3821	38.21	10.08	27.86	29.72
20.67	31.58	32.54	24.29	27.25	0.905	32.34	12.75	6.37	7.2	2902	29.02	15.39	29.24	23.69
19.25	31.62	32.87	25.42	27.29	0.749	34.89	17.58	16.74	9.02	2497	24.97	19.27	19.9	30.73
39.62	31.67	33.03	25.67	27.42	0.841	28.08	15.57	7.72	8.37	4105	41.05	17.8	26.8	32.99
34.54	31.87	33.17	25.83	27.62	0.529	17.26	14.62	11.98	22.98	3564	35.64	21.83	13.63	24.27
30	33.79	33.24	25.87	27.87	0.749	15.99	10.91	14.3	12.44	3047	30.47	17.26	18.03	15.57
22.92	33.96	33.29	26.58	28.25	1.011	24.38	12.8	4.88	15.99	2440	24.4	16.82	25.11	17.26
48.12	34	33.58	26.92	28.58	0.905	30.18	14.81	9.54	11.39	4040	40.4	16.95	22.1	14.4
16.04	34.17	34.12	27.12	28.79	0.675	21.34	19.09	8.41	14.9	2183	21.83	24.27	24.4	27.46
18.58	34.96	34.29	27.5	29.08	0.69	25.17	16.82	6.75	10.59	2326	23.26	25.96	28.77	24.73
24.58	35.12	34.5	28.29	29.42	0.592	15.09	16.76	14.25	15.99	3018	30.18	21.08	19.27	26.64

27.71	35.67	34.92	29.12	30.37	0.609	16.93	15.93	11.98	13.39	3127	31.27	23.45	14.62	15.99
38.71	35.87	35.42	29.87	30.46	0.837	25.13	17.07	12.78	10.04	3850	38.5	22.74	13.73	26.16
17.75	36.33	35.89	31.08	31.5	0.71	20.43	10.08	14.45	7.9	2183	21.83	31.82	12.58	35.95
14.75	36.67	37	31.12	31.58	0.794	21.39	14.62	11.39	7.15	1859	18.59	23.82	13.42	12.19
15.25	37.42	37.21	31.12	31.62	0.854	15.39	13.08	6.7	8.74	1766	17.66	21.71	26	17.07
46.17	37.67	37.42	31.67	31.67	0.72	17.66	13.8	7.9	22.62	4370	43.7	15.27	24.4	27.61
24.08	37.75	38.04	31.71	31.79	0.758	18.81	17.24	10.08	7.9	2690	26.9	19.09	20.11	32.31
26.75	38.5	38.7	32.75	32.42	0.79	21.97	10.88	7.72	7.49	3205	32.05	24.29	28.41	28.06
19.67	39.25	38.95	33.08	33.33	0.654	26	10.91	14.25	7.9	3033	30.33	32.66	31.14	47.92
30.42	39.37	39.32	34.17	33.37	0.654	17.6	17.6	20.11	9.02	4109	41.09	23.63	22.6	37.33
23.04	39.71	39.67	36.46	34.37	0.71	23.5	20.67	14.23	9.36	2497	24.97	33.34	12.56	48.56
18.79	40.17	42.25	36.5	34.42	0.824	18.81	14.21	13.73	8.41	2397	23.97	14.23	20.16	45.97
16.83	40.25	42.96	36.67	35.08	0.529	18.43	11.98	12.67	8.37	2152	21.52	18.43	17.26	38.84
27.83	40.58	43.41	37.29	36.37	0.758	30.24	15.64	16.57	8.62	3482	34.82	20.71	20.72	30.73
19.62	40.83	43.42	37.75	36.58	0.675	12.44	15.9	15.93	10.91	2524	25.24	31.91	19.27	25.31
20.71	41.87	43.75	37.83	36.75	0.854	20.23	10.49	13.5	16.51	2433	24.33	36.31	21.76	74.34
22.42	41.92	44.25	38.08	39.12	0.715	20.98	12.67	11.75	10.35	2861	28.61	49.39	15.07	44.65
17.12	42.12	44.83	38.25	39.58	0.609	18.43	10.72	13.23	11.17	2254	22.54	15.79	22.54	34.41
16.04	43.17	45.4	39.21	40.92	0.609	24.89	14.25	14.9	10.91	2397	23.97	19.7	20.79	19.61
13.67	43.21	47.33	39.21	41.58	0.637	24.73	13.86	10.72	9.76	2433	24.33	24.1	15.57	11.66
24.33	43.25	50.08	39.25	41.92	0.675	23.81	16.76	14.81	10.08	2370	23.7	20.09	15.43	18.28
17.21	43.25	51.1	39.5	42.04	0.71	25.84	11.98	7.72	12.56	2497	24.97	20.67	10.04	20.11
19.33	43.87	52.46	40.21	42.33	0.715	23.26	12.75	19.27	13.08	2489	24.89	18.03	22.62	24.72
20.12	43.92	53.87	40.96	42.42	0.69	17.66	13.63	9.36	9.05	2315	23.15	15.43	10.08	37.38
34.54	44.58	57.29	41.08	45.5	0.921	28.77	11.01	6.7	9.36	3615	36.15	21.83	6.7	51.09
30.71	44.58	59.79	41.79	45.75	0.794	24.29	18.43	6.37	9.36	3111	31.11	20.94	35.52	52.14
26.21	44.87	59.83	42.25	48.12	0.675	25.51	15.57	8.9	10.49	3024	30.24	19.97	34.65	20.99
15.42	45.12	62.08	42.5	49.33	0.604	16.17	15.37	8.37	9.36	2327	23.27	19.11	42.72	27.74
13.62	46.37	69.05	43.04	49.54	0.715	24.79	8.54	8.37	7.58	2210	22.1	8.41	34.89	36.08
22.75	46.42	72.12	43.42	50.96	0.586	29.72	9.25	7.15	8.37	2595	25.95	9.21	25.42	29.3
23.29	47.33	79.26	44.71	51.37	0.609	29.34	16.1	7.94	9.21	3303	33.03	19.11	31.52	32.64
31.92	50.25	85.25	46.96	52.21	0.753	25.62	20.99	13.93	8.24	3348	33.48	21.91	23.69	33.03
32.67	50.42	93.71	49.12	54.21	0.67	23.69	17.6	14.62	10.08	3348	33.48	20.16	18.81	35.79
23.17	50.62	102.41	50.62	56.42	0.758	25.11	12.07	9.54	7.9	3282	32.82	18.81	14.9	23.03

28.58	53.96	117.01	51.5	75.42	0.841	21.76	12.44	7.1	9.36	3365	33.65	20.16	30.47	22.62
26.17	54.62	119.86	62	139.04	0.837	17.24	13.52	8.62	11.26	2767	27.67	17.24	29.2	38.48
23.62	54.87	54.87	83.62	54.87	0.925	13.52	12.75	9.02	12.75	2684	26.84	13.52	33.48	13.52
23.71	57.67	57.67	57.67	57.67	0.874	27.71	20.67	20.67	20.67	2725	27.25	27.71	27.71	27.71
0.0271	57.83	57.83	57.83	57.83	0.837	17.91	15.39	15.39	15.39	837	8.37	17.91	17.91	17.91
45.67	59.75	59.75	59.75	59.75	0.837	21.83	15.57	15.57	15.57	4082	40.82	21.83	21.83	21.83
26.08	59.96	59.96	59.96	59.96	0.758	21.44	15.57	15.57	15.57	3125	31.25	21.44	21.44	21.44
20.54	64.17	64.17	64.17	64.17	0.609	17.17	15.57	15.57	15.57	2643	26.43	17.17	17.17	17.17
18.75	67.37	67.37	67.37	67.37	0.529	28.61	17.66	17.66	17.66	2808	28.08	28.61	28.61	28.61
15.12	12.17	5.83	5.42	6.42	0.609	33.79	20.39	10.84	11.06	2584	25.84	27.44	37.01	27.21
12.92	12.25	7.33	8.21	8	0.529	31.8	22.03	10.55	11.8	1932	19.32	28.06	33.82	21.9
13.96	13.25	7.67	8.67	8.33	0.837	26.23	12.31	10.33	8.88	1645	16.45	52.54	36.13	25.81
19.37	14.46	11.04	9.37	11.5	0.536	13.82	11.95	10.55	8.4	3198	31.98	24.49	29.16	25.03
34.37	15.71	12.42	9.92	12.33	0.536	26.54	20.52	7.78	15.64	4150	41.5	58.43	32.51	18.24
19.5	15.96	15.12	10.33	12.37	0.609	31.49	43.02	16.48	16.99	2861	28.61	57.19	25.67	17.33
32.21	16.17	16.87	10.83	12.58	0.529	33.88	23.82	10.71	8.88	4043	40.43	38.59	37.59	14.6
14.25	16.25	17.5	10.87	13.25	0.637	17.42	23.87	9.61	11.06	2246	22.46	22.23	28.17	19.59
26.71	17.29	18.25	11.67	13.79	0.654	14.64	14.12	14.08	6.8	3677	36.77	18.72	22.9	31.38
25.12	18	18.33	11.75	14.75	0.474	19.27	12.2	14.04	7.78	3484	34.84	26.13	29.77	25.28
17.87	18.17	18.42	11.79	14.83	0.604	27.25	16.17	7.42	5.53	2445	24.45	28.31	49.07	26.19
15.58	18.79	18.46	12	15.5	0.302	26.07	23.51	13.31	6.64	2546	25.46	67.19	22.5	42.19
0.0904	18.96	18.58	12	15.92	0.592	14.25	16.42	11.8	6.8	1898	18.98	36.98	41.19	31.2
27.21	19.17	18.58	13	17.33	0.509	18.36	8.57	22.27	5.83	4500	45	19.99	38.98	23.21
24.83	21	19	13.58	17.33	0.637	26.79	10.67	9.92	9.92	3047	30.47	30.85	50.46	22.39
19.79	21.08	19.04	14.21	17.37	0.536	22.85	17.42	11.8	7.6	2696	26.96	26.13	31.55	22.9
14.21	21.21	19.42	14.33	17.5	0.79	22.98	15.14	10.06	5.94	2139	21.39	30.21	22.9	21.77
21.42	21.29	19.75	14.37	17.62	0.592	19.54	9.03	16.69	7.37	2949	29.49	38.66	22.9	19.4
21.33	21.37	19.75	14.96	17.67	0.604	23.15	28.92	19.29	5.94	2620	26.2	69.01	23.6	27.7
26.37	21.58	19.83	14.96	18.04	0.69	14.9	14.69	8.9	9.21	3151	31.51	35.91	29.81	27.64
29.17	21.67	20.33	15.08	18.12	0.592	25.55	10.33	8.41	7.42	3334	33.34	18.43	26.16	25.6
26.42	22.75	20.54	15.21	18.17	0.824	22.54	16.48	7.58	9.65	3264	32.64	20.8	18.72	28.95
24.54	23.29	20.67	15.25	18.25	0.562	31.81	14.39	7.15	10.06	2891	28.91	24.35	28.91	43.71
28.83	24	21.08	15.29	18.87	0.902	26.8	19.22	8.37	5.21	4050	40.5	58.28	25.79	19.12

20.29	24.04	21.54	15.33	19.67	0.69	30.47	13.52	6.04	7.37	3311	33.11	33.64	23.45	21.19
30.12	24.33	21.62	15.79	20.04	0.67	25.79	19.95	6.54	5.53	3516	35.16	32.06	21.13	38.63
21.29	24.83	21.71	16.04	20.46	0.509	27.16	22.42	7.15	12.55	2762	27.62	40.72	20.38	17.46
34.58	24.92	21.87	16.29	20.54	0.753	25.55	18.24	6.37	7.46	3564	35.64	40.28	42.68	14.86
23.96	25.17	21.96	17.33	20.67	0.67	22.16	21.63	9.54	8.6	3098	30.98	27.11	14.97	14.39
31.58	25.54	22.33	17.87	20.92	0.562	19.76	14.86	7.72	20.93	3155	31.55	18.97	26.47	27.64
24.25	25.58	22.92	17.92	21.08	0.675	27.74	14.23	7.2	19.54	2737	27.37	25.39	19.97	23.5
19.33	26.21	23.04	18	21.67	0.536	21.6	24.73	6.9	11.84	2315	23.15	43.69	49.28	12.99
12.92	26.5	23.37	18.12	22	0.536	18.98	21.76	6.37	16.95	1954	19.54	31.55	22.24	20.43
21.58	26.71	23.75	18.67	22.58	0.654	14.64	25.11	6.37	18.72	2832	28.32	27.82	32.57	20.93
23.96	26.83	23.96	18.87	22.62	0.654	30.71	13.93	5.62	10.22	3138	31.38	28.8	21.97	22.1
16.75	26.96	24.04	19.5	22.96	0.609	11.39	16.93	9.25	12.56	1959	19.59	25.24	36.61	18.42
16.87	27.46	25.58	19.83	23.04	0.562	16.76	7.72	6.37	9.54	2197	21.97	15.88	15.37	33.9
38.96	27.46	26.33	20.04	23.04	0.772	23.35	9.05	7.72	8.29	4295	42.95	14.25	17.07	44.37
15.87	27.46	26.38	20.75	23.67	0.675	21.6	7.15	10.04	8.37	2508	25.08	7.72	41.85	21.34
24.33	27.58	26.46	20.87	23.75	0.772	18.81	20.16	9.21	9.76	2901	29.01	26.8	34.48	17.26
29.83	28.08	26.67	21.67	24.25	0.71	22.54	12.56	9.21	11.39	3018	30.18	16.57	36.98	19.9
31.54	28.12	26.75	21.92	24.33	0.772	30.32	18.81	17.89	7.58	3623	36.23	22.11	17.07	22.16
24.46	28.58	26.83	21.96	24.46	0.592	39.7	10.65	13.08	12.75	2949	29.49	17.76	13.08	12.75
19.54	28.62	27.08	22.21	24.5	0.829	22.62	11.39	16.85	10.18	2315	23.15	14.21	18.03	31.52
21.42	29.21	28.42	22.5	26	0.374	29.31	16.68	7.9	14.33	3303	33.03	14.03	10.91	42.15
22.71	29.21	28.54	23.08	26	0.536	17.76	11.23	13.23	9.05	2489	24.89	19.09	13.08	40.19
20.29	29.67	28.62	23.67	26	0.609	16.85	11.9	9.47	8.9	2472	24.72	17.97	11.66	26.96
33.96	30.08	28.87	23.75	26.12	0.71	24.79	10.59	6.37	5.92	3935	39.35	18.88	10.35	25.79
22.92	30.33	29	23.79	26.17	0.637	25.85	10.59	7.2	5.62	3111	31.11	12.99	28.57	30.33
21.21	30.5	29.12	23.79	26.33	0.637	25.13	13.08	5.86	11.39	2675	26.75	21.34	20.11	29.28
27.46	30.71	29.46	24.04	26.54	0.637	25.55	10.91	8.62	8.24	3638	36.38	24.1	39.23	28.47
25.67	30.92	29.58	24.17	26.75	0.715	16.74	10.49	9.54	9.02	3870	38.7	16.51	33.9	41.15
23.33	30.96	30.17	24.25	26.87	0.69	18.43	17.26	9.47	5.92	3289	32.89	23.03	40.53	55.49
29	31.46	30.29	24.25	27.12	0.837	23.5	10.65	6.54	8.29	3334	33.34	10.08	27.86	29.72
33.67	31.58	32.54	24.29	27.25	0.654	32.34	12.75	6.37	7.2	3805	38.05	15.39	29.24	23.69
22.04	31.62	32.87	25.42	27.29	0.654	34.89	17.58	16.74	9.02	2782	27.82	19.27	19.9	30.73
18.12	31.67	33.03	25.67	27.42	0.654	28.08	15.57	7.72	8.37	2486	24.86	17.8	26.8	32.99
28.67	31.87	33.17	25.83	27.62	0.71	17.26	14.62	11.98	22.98	3447	34.47	21.83	13.63	24.27

26.29	33.79	33.24	25.87	27.87	0.586	15.99	10.91	14.3	12.44	3850	38.5	17.26	18.03	15.57
31.5	33.96	33.29	26.58	28.25	0.592	24.38	12.8	4.88	15.99	4268	42.68	16.82	25.11	17.26
27.42	34	33.58	26.92	28.58	0.586	30.18	14.81	9.54	11.39	3683	36.83	16.95	22.1	14.4
0.00058	34.17	34.12	27.12	28.79	0.758	21.34	19.09	8.41	14.9	2262	22.62	24.27	24.4	27.46
11.92	34.96	34.29	27.5	29.08	0.675	25.17	16.82	6.75	10.59	1959	19.59	25.96	28.77	24.73
17.17	35.12	34.5	28.29	29.42	0.536	15.09	16.76	14.25	15.99	2886	28.86	21.08	19.27	26.64
17.33	35.67	34.92	29.12	30.37	0.654	16.93	15.93	11.98	13.39	2620	26.2	23.45	14.62	15.99
22.5	35.87	35.42	29.87	30.46	0.529	25.13	17.07	12.78	10.04	3251	32.51	22.74	13.73	26.16
18.54	36.33	35.89	31.08	31.5	0.749	20.43	10.08	14.45	7.9	1881	18.81	31.82	12.58	35.95
19.67	36.67	37	31.12	31.58	0.749	21.39	14.62	11.39	7.15	2113	21.13	23.82	13.42	12.19
38.79	37.42	37.21	31.12	31.62	0.837	15.39	13.08	6.7	8.74	3869	38.69	21.71	26	17.07
29.87	37.67	37.42	31.67	31.67	0.675	17.66	13.8	7.9	22.62	3282	32.82	15.27	24.4	27.61
34.79	37.75	38.04	31.71	31.79	0.675	18.81	17.24	10.08	7.9	3622	36.22	19.09	20.11	32.31
35.54	38.5	38.7	32.75	32.42	0.749	21.97	10.88	7.72	7.49	3833	38.33	24.29	28.41	28.06
47.83	39.25	38.95	33.08	33.33	0.89	26	10.91	14.25	7.9	4812	48.12	32.66	31.14	47.92
17	39.37	39.32	34.17	33.37	0.592	17.6	17.6	20.11	9.02	2368	23.68	23.63	22.6	37.33
26.04	39.71	39.67	36.46	34.37	0.837	23.5	20.67	14.23	9.36	2863	28.63	33.34	12.56	48.56
16	40.17	42.25	36.5	34.42	0.654	18.81	14.21	13.73	8.41	2079	20.79	14.23	20.16	45.97
23.87	40.25	42.96	36.67	35.08	0.675	18.43	11.98	12.67	8.37	2473	24.73	18.43	17.26	38.84
19.04	40.58	43.41	37.29	36.37	0.609	30.24	15.64	16.57	8.62	2518	25.18	20.71	20.72	30.73
22.79	40.83	43.42	37.75	36.58	0.675	12.44	15.9	15.93	10.91	3098	30.98	31.91	19.27	25.31
32.75	41.87	43.75	37.83	36.75	0.794	20.23	10.49	13.5	16.51	4266	42.66	36.31	21.76	74.34
29.58	41.92	44.25	38.08	39.12	0.529	20.98	12.67	11.75	10.35	4215	42.15	49.39	15.07	44.65
23.92	42.12	44.83	38.25	39.58	0.925	18.43	10.72	13.23	11.17	2959	29.59	15.79	22.54	34.41
30.71	43.17	45.4	39.21	40.92	0.715	24.89	14.25	14.9	10.91	2924	29.24	19.7	20.79	19.61
30.21	43.21	47.33	39.21	41.58	0.837	24.73	13.86	10.72	9.76	2930	29.3	24.1	15.57	11.66
20.75	43.25	50.08	39.25	41.92	0.79	23.81	16.76	14.81	10.08	2414	24.14	20.09	15.43	18.28
23.08	43.25	51.1	39.5	42.04	0.654	25.84	11.98	7.72	12.56	2746	27.46	20.67	10.04	20.11
24.92	43.87	52.46	40.21	42.33	0.675	23.26	12.75	19.27	13.08	4253	42.53	18.03	22.62	24.72
30.58	43.92	53.87	40.96	42.42	0.837	17.66	13.63	9.36	9.05	3851	38.51	15.43	10.08	37.38
20.58	44.58	57.29	41.08	45.5	0.772	28.77	11.01	6.7	9.36	2379	23.79	21.83	6.7	51.09
16.08	44.58	59.79	41.79	45.75	0.654	24.29	18.43	6.37	9.36	2134	21.34	20.94	35.52	52.14
19.12	44.87	59.83	42.25	48.12	0.749	25.51	15.57	8.9	10.49	2369	23.69	19.97	34.65	20.99
19.	45.1	62.08	42.5	49.33	0.794	16.1	15.37	8.37	9.36	2397	23.9	19.11	42.72	27.74

33	2					7					7			
35.17	46.37	69.05	43.04	49.54	0.925	24.79	8.54	8.37	7.58	4465	44.65	8.41	34.89	36.08
38.87	46.42	72.12	43.42	50.96	0.841	29.72	9.25	7.15	8.37	4021	40.21	9.21	25.42	29.3
47.29	47.33	79.26	44.71	51.37	0.654	29.34	16.1	7.94	9.21	4505	45.05	19.11	31.52	32.64
36.21	50.25	85.25	46.96	52.21	0.772	25.62	20.99	13.93	8.24	4040	40.4	21.91	23.69	33.03
32.87	50.42	93.71	49.12	54.21	0.749	23.69	17.6	14.62	10.08	3743	37.43	20.16	18.81	35.79
	50.62	102.41	50.62	56.42		25.11	12.07	9.54	7.9			18.81	14.9	23.03
	53.96	117.01	51.5	75.42		21.76	12.44	7.1	9.36			20.16	30.47	22.62
	54.62	119.86	62	139.04		17.24	13.52	8.62	11.26			17.24	29.2	38.48
	54.87	54.87	83.62	54.87		13.52	12.75	9.02	12.75			13.52	33.48	13.52
	57.67	57.67	57.67	57.67		27.71	20.67	20.67	20.67			27.71	27.71	27.71
	57.83	57.83	57.83	57.83		17.91	15.39	15.39	15.39			17.91	17.91	17.91
	59.75	59.75	59.75	59.75		21.83	15.57	15.57	15.57			21.83	21.83	21.83
	59.96	59.96	59.96	59.96		21.44	15.57	15.57	15.57			21.44	21.44	21.44
	64.17	64.17	64.17	64.17		17.17	15.57	15.57	15.57			17.17	17.17	17.17
	67.37	67.37	67.37	67.37		28.61	17.66	17.66	17.66			28.61	28.61	28.61